

2015-2018

China National Report on Geodesy

For

The 27th IUGG General Assembly

Montréal, Québec, Canada, July 8-18, 2019

Prepared by Chinese National Committee for
International Association of Geodesy (CNC-IAG)

June 25 2019

Contents

Preface.....	1
1. Construction and Service of modern geodetic datum and reference frame in China.....	2
1.1 Introduction.....	2
1.2 Construction of Modern National surveying and mapping datum project.....	3
1.3 The development of CGCS2000.....	5
1.3.1 CGCS2000 putting into full application.....	5
1.3.2 Study on nonlinear movement of China Coordinate frame.....	5
1.3.3 Study on epoch reference frame establishment.....	5
1.4 Construction and Service of National dynamic geocentric coordinate reference framework.....	6
1.5 BDS/GNSS data processing and analysis.....	7
1.5.1 Introduction to BeiDou Navigation Satellite System (BDS).....	7
1.5.2 GNSS monitoring & assessment.....	8
1.5.3 GNSS products and its development.....	11
1.5.4 Positioning performance and improvement.....	13
1.6 Development on the seafloor geodetic network.....	17
2. Earth gravity field and height datum.....	25
2.1 Earth gravity field.....	25
2.2 Height datum and geoid model.....	29
2.3 Time variable gravity and related application.....	34
2.3.1 Post-processing method.....	34
2.3.2 Terrestrial water storage variants monitoring.....	35
2.3.3 Sea level change and Extreme climate monitoring.....	36
2.3.4 Load deformation motoring.....	37
2.3.5 Low degree and geocenter motion study.....	38
2.3.6 Effect factors analysis and geophysical interpretation.....	39
2.4 Satellite altimetry.....	41
2.4.1 Method.....	41
2.4.2 Data Processing.....	42
2.4.3 Applications.....	43
3. Positioning and Application.....	54
3.1 Comprehensive PNT architecture.....	54
3.2 BDS Triple-frequency PPP.....	56
3.3 Triple-frequency observations analysis.....	57
3.4 Indoor Positioning.....	58
4. Researches and Application of Chinese Geodetic Observing System.....	61
4.1 Data processing method.....	61
4.2 Monitoring of water storage variants and deformation.....	62
4.3 Geodetic inversion.....	63
4.4 Seismological applications of geodesy.....	64

Preface

This report presents the progress of research and development on geodesy in China during the time period from January 2015 to December 2018. It is to be submitted, on behalf of the Chinese National Committee for International Association of Geodesy (CNC-IAG), to the IAG General Assembly at the 27th IUGG General Assembly to be held in Montréal, Québec, Canada, July 8-18, 2019.

The report includes the following contents:

1. Construction and Service of modern geodetic datum and reference frame in China
2. Earth gravity field and height datum
3. Positioning and Application
4. Researches and Application of Chinese Geodetic Observing System

It is hoped that this national report would be of help for Chinese scientists in exchanging the results and ideas in the research, development and application of geodesy with scientists all over the world.

Colleagues listed below made their contribution for this national report (in alphabetical order):

BIAN Shaofeng, CHENG Pengfei, CHENG Yingyan, CHEN Ruizhi, DANG Yamin, DENG Zhongliang, GENG Jianghui, HUANG Motao, JIANG Weiping, JIN Shuanggen, JIANG Tao, KE Baogui, LI Dehai, LIU Jingnan, LU Zhiping, LI Bofeng, LUO Zhicai, LI Jiancheng, LI Zhiwei, SUN Zhongmiao, SHEN Yunzhong, SHEN Wenbin, WANG Wei, WANG Hu, WANG Min, WU Xiaoping, XU Caijun, XU Tianhe, XU Changhui, XUE Shuqiang, YANG Yuanxi, YANG Qiang, YAO Yibin, YU Baoguo, YU Jinhai, YUAN Yunbin, ZHANG Chuanyin, ZHANG Xiaohong, ZHU Jianjun, ZHANG Qin, ZHAO Jianhu.

Prof. DANG Yamin
President of CNC-IAG

1. Construction and Service of modern geodetic datum and reference frame in China

1.1 Introduction

The 1954 Beijing coordinate system and the 1954 Xi'an coordinate system established in the last century using astronomical geodetic surveying calibration and adopted reference ellipsoid coordinate systems, has played an important role in the economic construction and national defense construction in China (Chen Jun-yong 2007, 2008; Zhu Hua-tong, 1990). However, these two coordinate systems belong to regional reference ellipsoid coordinate system with the disadvantage of low surveying precision and it is difficult to meet the needs of national defense, economic construction and scientific research. Therefore, many scholars proposed to build a new generation of China geocentric coordinate system (Chen Jun-yong 1999; Gu Dan-sheng, 2003; Wei Zi-qing, 2003; Yang Yuan-xi 2005) and carried out theory and practical research in depth. The related researches include: Characteristics of annual and semiannual movement variations of reference framework stations (Zhu Wen- yao,2003); Method for establishing the velocity field model of crustal movement in China (Liu Jing-nan, Shi Chuang, Yao Yi-bin 2002); Reflection the non-linear crustal movement of reference framework stations using global weeks solution(Gu Guo-hua,2006;Zhang Xi-guang,2009); Construction of China geodetic coordinate system 2000, Velocity field and plate motion model in mainland China(Wei Zi-qing,2011;Cheng Peng-fei, Cheng Ying-yan,2011;LV Zhi-ping,2013); Establishment and maintenance of terrestrial reference frame considering non-linear variation(Jiang Wei-ping, 2010);Initial realization and analysis of Compass terrestrial reference frame(Liu Jing-nan,2009;Wei Na,2013;Zou Rong,2011); Creation of a new generation of geodetic GGOS products using fusing a variety of geodetic observations and technical methods(Dang Ya-min,2006), etc.

To promote and maintain CGCS2000, a unified geometric and vertical datum with high accuracy, three dimensional, dynamic system should be established for China in the near future. The National Administration of Surveying, Mapping and Geoinformation and related scientific research institution in China have been carrying out datum research on the national level. The specific works are as follows:

Construction and service of modern geodetic datum and reference frame in China (National surveying and mapping datum project) of China's 12th "five-year plan" is the largest national geographic space infrastructure projects in China to maintain the national geodetic coordinate frame so far. Since the implementation of National surveying and mapping datum project from June 2012, five items of projects (National GNSS continuously operating reference station network

construction, National GNSS geodetic network, National elevation control network, National gravity datum points, and National surveying and mapping data system construction) have gradually built up surveying and mapping infrastructure with stable foundation, reasonable distribution, conducive to long-term preservation through ways of building, rebuilding and using. With the smooth implementation of surveying and mapping project, national modern geodetic datum system has been gradually established with the characteristic of high precision, covering all land and sea, three-dimensional, and dynamic. A geometric datum and vertical datum of high accuracy, three-dimensional, dynamic system of the modern geodetic datum will be built eventually, providing the service supporting capability for national modern economic construction, national defense construction and scientific research, etc.

1.2 Construction of Modern National surveying and mapping datum project

The “National surveying and mapping datum project” is a project that integrates geodetic datum infrastructure, height datum infrastructure and gravity datum infrastructure as a whole. The project used satellite technology, leveling surveying, gravity measurement, information systems, and other technical methods to build a modern geodetic datum, height datum and gravity datum infrastructure with reasonable density and uniform distribution, as well as national surveying and mapping datum management service system. By establishing and maintaining mutually complementary and interdependent surveying and mapping datum infrastructure, finally establish a system with national modern surveying and mapping benchmark data, results management and integrated services capabilities.

Through the update and perfect infrastructure, the objective of national modern surveying and mapping system construction will be achieved. The specific works are as follows:

- 1) 360 national GNSS continuous operation reference stations built all over the country, which will constitute the backbone of our country’ s national coordinate system framework(150 new stations; 60 transform station);
- 2) 4500 points of national GNSS geodetic control network built all over the country, which will relatively evenly cover the entire land area with reasonable density and wider range of service (2500 new points).
- 3) The first class leveling network will be comprehensively updated, including 775 new basic leveling points, 7030 ordinary leveling points, 110 leveling points on the bedrock and 27400 gravity points;
- 4) 50 gravity points will be selected on the national GNSS continuously operating reference stations, and the absolute gravity properties will be determined at 100 points to expand

the distribution and service area of national gravity datum.

5) Complete computer room renovation, network communication, computer and storage backup, security system and other operational supporting environment construction, as well as data management, processing, analysis and sharing service system, update the national surveying and mapping benchmark management service system.

1.3 The development of CGCS2000

1.3.1 CGCS2000 putting into full application

China government has public released to stop use 1954 Beijing Coordinate System and 1980 Xian Coordinate System since 1 January 2019. Up to present, most products of surveying and mapping related to the previous coordinate systems have been transformed to CGCS2000. The newly produced products of surveying and mapping are all based in CGCS2000. On the other hand, all CORS coordinates determined in later ITRFs in China area (different from ITRF97) at current epoch, based grid velocity, were then transformed to CGCS2000.

1.3.2 Study on nonlinear movement of China Coordinate frame

As to China coordinate frame maintenance , Because many GPS time series contain offsets, sometimes nonsecular trends, and seasonal signals with time-varying amplitudes due to several different types of geophysical phenomena. China scientists conduct some research on site nonlinear movement modelling. An enhanced singular spectrum analysis (SSA) method for fitting GPS time series and singular spectrum analysis for prediction (SSA-P), are proposed, the latter is used to establish forecast model for CGCS2000. Simulation results show that the root-mean-square (RMS) of differences between the reconstructed and simulated signals is 1.7 mm; the RMS of the differences between the predicted coordinates and simulated signal is about 3mm for the first half 1.5 years of testing period and decreases to 10mm for the last half 1.5 years. Meanwhile Singular spectrum analysis for missing data (SSA-M) and Singular Spectrum Analysis-Inter Quartile (SSA-IQR), are used for pretreatment of GPS time series. Establishing Non-linear model of CGCS2000 framework can improve the precision of domestic coordinate system, which can provide support for precise orbit determination of Beidou satellites and precise point positioning.

1.3.3 Study on epoch reference frame establishment

The linear velocity provided by ITRF cannot truly reflect the position change of the station, especially is not enough to reflect seasonal or short-term changes. China scientists made some research and build on the epoch reference framework to compensate for the lack of ITRF's linear speed, and the GNSS, SLR, VLBI technology SINEX file is used as the input data to reconstruct the unconstrained equations to realize multi-source data combination and solve the station coordinates and ERP parameters at the same time, and construct a multi-technology epoch reference frame. Verify the accuracy of ERP parameters and coordinates of the multi-technology based epoch reference frame by comparing with ERP value derived from single-technology, and with real position time serials of China reference frame respectively.

1.4 Construction and Service of National dynamic geocentric coordinate reference framework

The national GNSS continuous operation reference stations are modern infrastructures for establishing and maintaining high-precision, dynamic, geocentric, and three-dimensional coordinate reference frames at national, provincial, and municipal levels. It is the core of the mapping datum system and the basic geospatial framework. Network planning is an important step in achieving a new generation of national high-precision spatial datum.

1) Construction and Service of National datum framework

The National Basic Geographic Information Center and the Chinese Academy of Surveying and Mapping have used 410 national CORS stations (210 Beidou) to carry out data analysis, monitoring, and evaluation. It can generate national reference frame service products and Beidou products (satellite orbit, satellite clock, earth rotation parameters, ionosphere, troposphere, and other reference products), maintain and update autonomous and controllable national coordinate framework, so that it can effectively meet the high-precision benchmark requirements of surveying and mapping and related industries, and promote the application of Beidou surveying and mapping geographic information and industrial development.

2) Construction and service of national and provincial unified datum framework

In order to unify the national coordinate framework, provide more scientific and accurate benchmark data, and further enhance the ability and level of economic and social development of surveying and mapping geographic information services, the ministry of natural resources has organized annual adjustment of national and provincial benchmark network since 2014. The observation data from 31 self-built provincial GNSS reference stations and reference engineering stations, 927 project GNSS reference stations and GNSS reference stations of crustal movement (a total of 1800 stations) observation network during 1th-31th August were calculated by the integral adjustment under the nationwide GNSS network. The National Basic Geographic Information Center, the Chinese Academy of Surveying and Mapping and the National Geodetic Data Processing Center carry out the national joint network calculation and overall adjustment, and obtain the results of precise geocentric coordinates under the national unified spatial benchmark, which can solve the problems of inconsistent coordinate frame of provincial reference stations network and inconsistent of navigation and positioning datum of provincial regions. The progress of the coordinate frame network will lay a good foundation for the maintenance of national dynamic geocentric coordinate reference framework.

1.5 BDS/GNSS data processing and analysis

1.5.1 Introduction to BeiDou Navigation Satellite System (BDS)

The BeiDou Navigation Satellite System (BDS) has been independently constructed and operated by China with an eye to the needs of the country's national security and economic and social development. As a space infrastructure of national significance, BDS provides all-time, all-weather and high-accuracy positioning, navigation and timing services to global users (<http://en.beidou.gov.cn/SYSTEMS/System/>).

China applies the principle that “BDS is developed by China, and dedicated to the world” and adheres to the BeiDou spirit of “independent innovations, unity and collaboration, overcoming difficulties, and the pursuit of excellence”. BDS provides the significant time and space information guarantee for economic and social development, and is one of the important achievements in the past 40 years of China's reform and opening-up, and serves as a public resource contributed by China to the world. China is willing to share the outcome of BDS construction and development with all other countries, to promote global satellite navigation development and make Global Navigation Satellite Systems (GNSS) better serve the world and benefit mankind (Development of the BeiDou Navigation Satellite System Version 3.0).

BDS is planned to comprehensively complete the BDS-3 deployment with the launching of 30 satellites by around 2020. By the 25st June, 2019, a total of 46 satellites including MEO, IGSO and GEO, had been launched to complete a preliminary system for global services.

BDS is mainly comprised of three segments: the space segment, the ground segment and the user segment. BDS augmentation systems, which contains ground-based and satellite-based, are developing to improve the performance of BDS. In order to monitor the BDS system operation and provide the services, International GNSS Monitoring & Assessment System (iGMAS) is established. It is consisted of 30 tracking stations distributed throughout the world, 3 Data Centers, 12 Analysis Centers, a Monitoring & Assessment Center, a Products Combination & Service Center and an Operation Control & Management Center. The main tasks of iGMAS are as below:

- 1) Establish a worldwide near-real-time tracking network for BDS/GPS/GLONASS/Galileo navigation satellite segment.
- 2) Build an information service platform for data collection, storage, analysis, management, publishment and any other functions.
- 3) Monitor and assess the operation status and key performance indicators of Global Satellite Navigation System (GNSS).

1.5.2 GNSS monitoring & assessment

The Monitoring & Assessment Center combine the data from data centers, Products Combination & Service Center and other data to monitoring and assessing the constellation status, navigation signals, message information and service performance. These information including constellation availability monitoring, space signals quality monitoring, navigation information and service monitoring, are provided to the public users (Fig. 1.1).

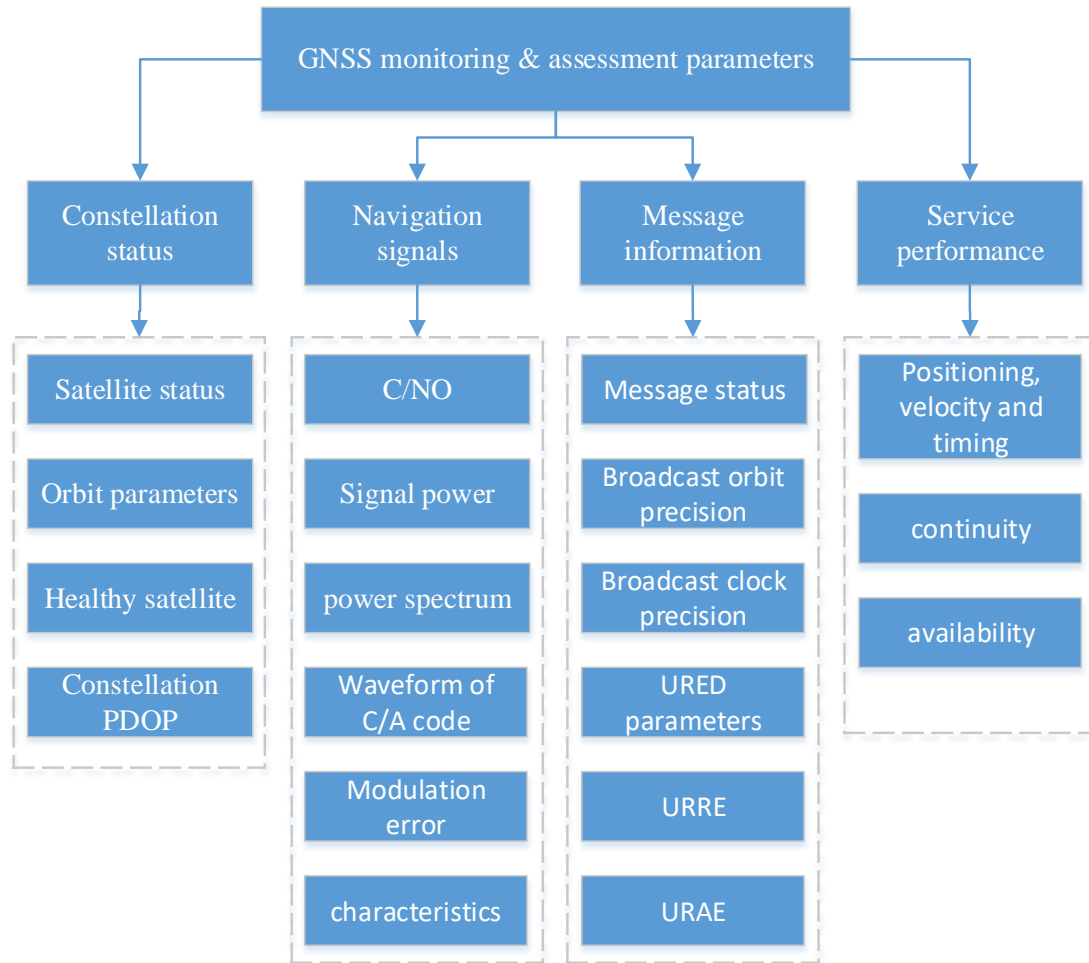


Fig. 1.1 GNSS monitoring and assessment

Signal-In-Space User Range Errors (SIS UREs) are assumed to be overbounded by a normal distribution with a standard deviation, which can be used for Receiver Autonomous Integrity Monitoring (RAIM) False Alert Probability (Pfa) and availability evaluation. The clock errors of the GEO and IGSO satellites change significantly, the clock stability of the MEO satellites is better than that of the IGSO and GEO satellites. The RMS of IGSO and MEO orbit error calculated from broadcast ephemeris is better than 3m and the RMS of GEO better than 5m. The mean SIS URE of GEO is less than 1.5m, its mean SIS URE of IGSO is less than 1.0m and that of MEO less than 0.5m (Wang, 2018; Cao, 2019; Ma, 2019; Liu, 2018).

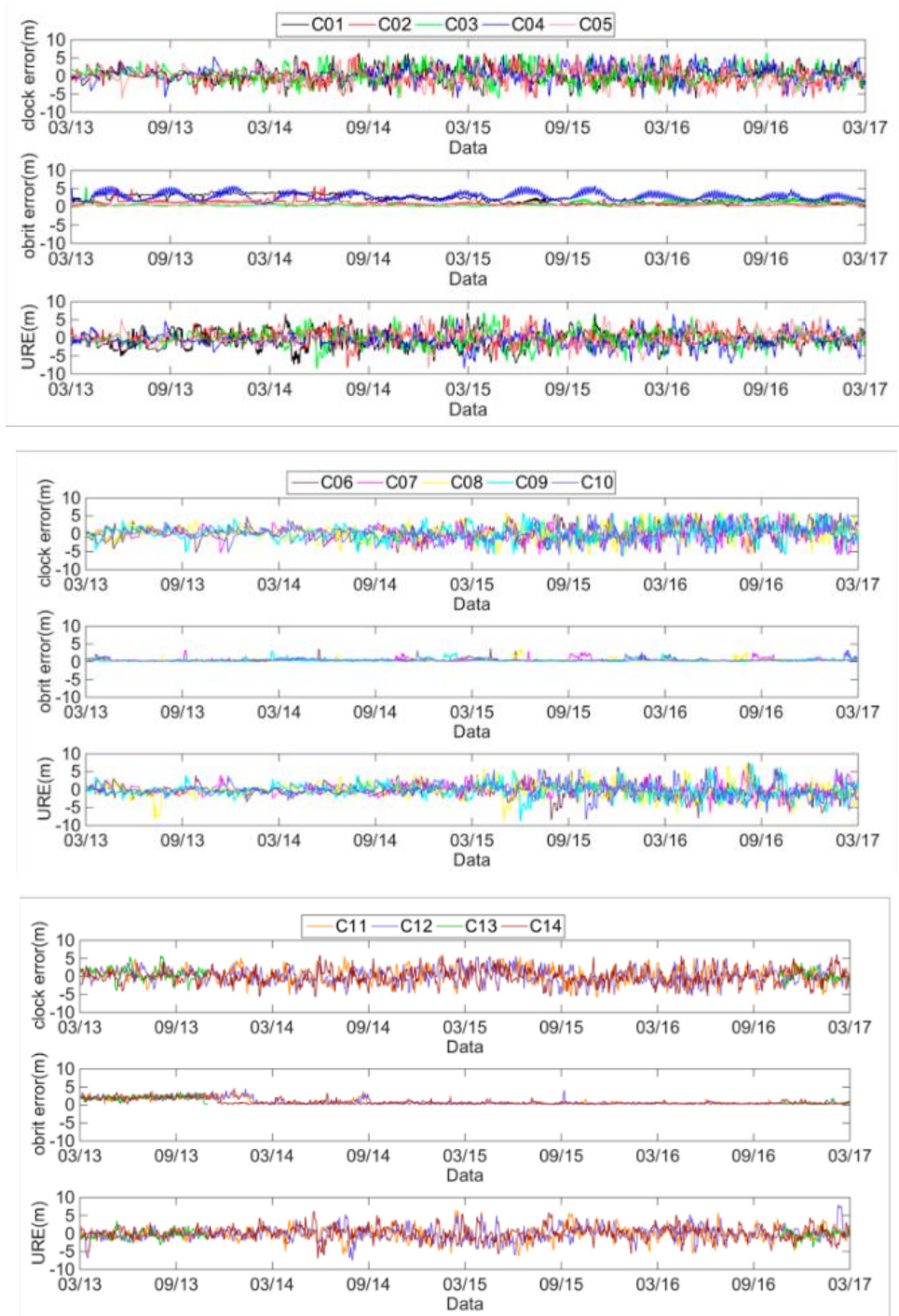


Fig. 1.2 Clock error, orbit error and URE

The carrier-to-noise density ratio (C/N_0) and its variation with elevation provides a key figure of merit for the characterization of the wide variety of signals accessible with modern receivers. Taking CHU1, CANB, and ICUK stations as examples, The observed C/N_0 values of GPS, Galileo (GAL), and BDS-2 and BDS-3 signals are depicted as a function of satellite elevation. The GPS L5 signals exhibit the highest C/N_0 values over the entire elevation range for each of the three stations. BDS-3 B1C signals exhibit the lowest C/N_0 values for the three stations. For compatible signals (B1I/B3I) of BDS-2 and BDS-3, the B1I signals of BDS-3 are approximately 3 dB-Hz more

powerful than those of BDS-2 for all three stations, while the B3I signals show almost the same C/N0 values for BDS-2 and BDS-3 (Xie, 2018).

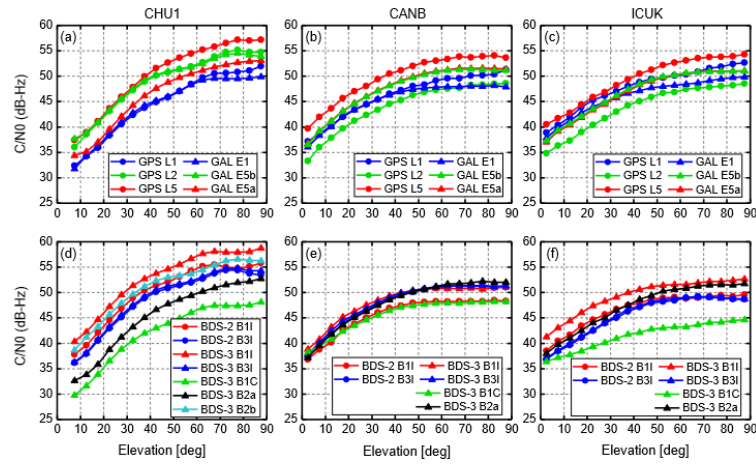


Fig. 1.3 Mean C/N0 values as a function of satellite elevation for all the available signals of GPS and Galileo (a-c) and BDS-2 and BDS-3 (d-f)

Monitoring & Assessment Center will also monitor the observed satellites' positions (Fig. 1.4) and their operation status (Fig. 1.5) real-time from the website (<http://www.igmas.org>). Every analysis center or other users can find the GNSS satellite information. At the same time, availability and PDOP (PDOP) of satellite at anytime is also provided, which can be used for surveying plan.

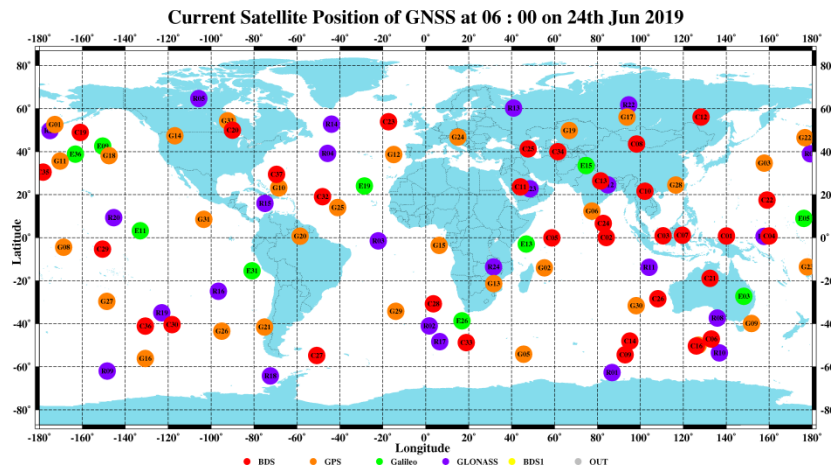


Fig. 1.4 Current satellite position of GNSS

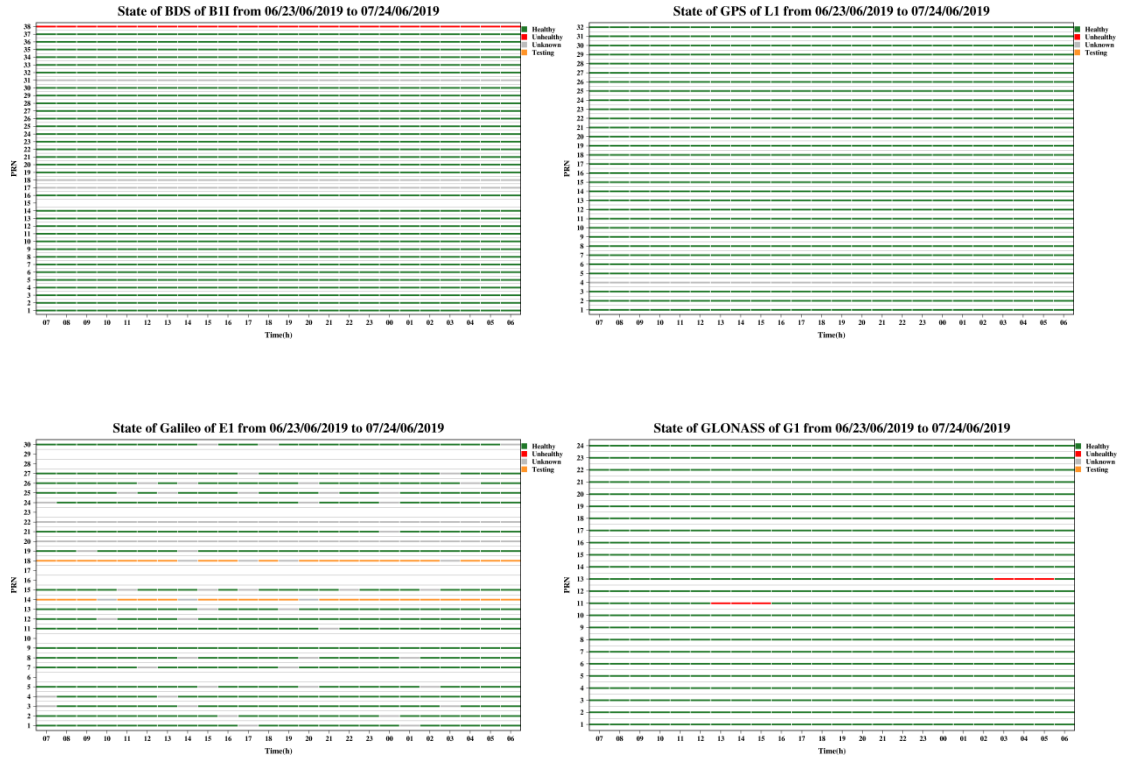


Fig. 1.5 State of GNSS

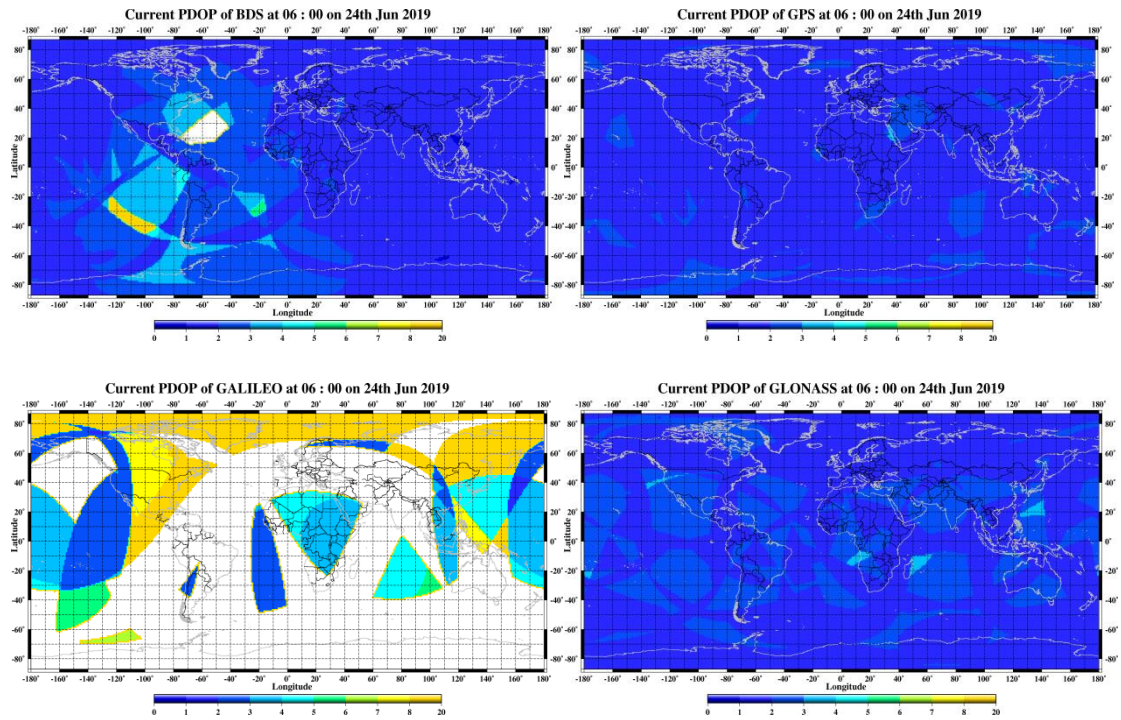


Fig. 1.6 PDOP

1.5.3 GNSS products and its development

Products Combination & Service Center will combine the products from 12 analysis center. These products are satellite precise orbit, precise clock, Earth-centered coordinates of tracking

stations, earth rotation parameters, ionosphere, troposphere, inter-frequency information and integrity products. Different orbit products (ultra-rapid (predicted), ultra-rapid (observed), rapid and final) have their precision, time delay and update time. These information can be found from the BDS official website. The precision of combined GPS final orbit is about 5mm and that of BDS is less than 20mm.

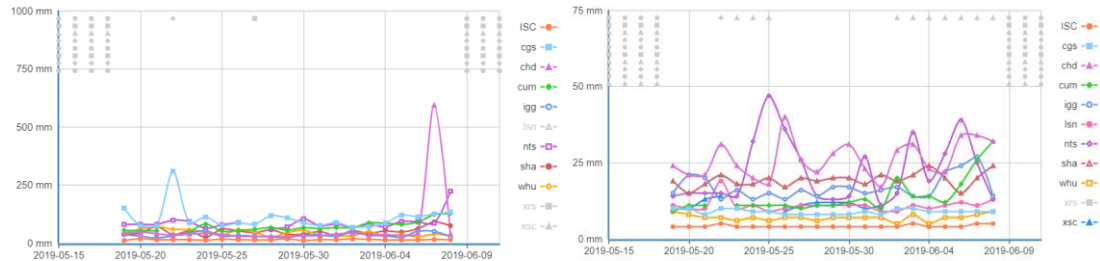


Fig. 1.7 Final GPS and BDS orbit products

The GNSS Occultation Sounder instrument onboard the Chinese meteorological satellite Fengyun-3C (FY-3C) tracks both GPS and BDS signals for orbit determination. POD of FY-3C is firstly performed with GPS data and then used as reference orbits for evaluating the orbit precision of GPS and BDS combined POD as well as BDS-based POD. It is indicated that inclusion of BDS geosynchronous orbit satellites (GEOs) could degrade POD precision seriously. The precision of orbit estimates by combined POD and BDS-based POD are 3.4 and 30.1 cm in 3D RMS when GEOs are involved, respectively. However, if BDS GEOs are excluded, the combined POD can reach similar precision with respect to GPS POD, showing orbit differences about 0.8 cm (Li, 2017). However, according to Li’s (2018) results, both BDS and GPS orbits present a significant improvement after including FY-3C data for a regional network, at the same time, the orbit precision of the BDS+GPS solution is improved by 4% for GPS, 5%, 16% and 19% for BDS GEO, IGSO and MEO respectively for a global network.

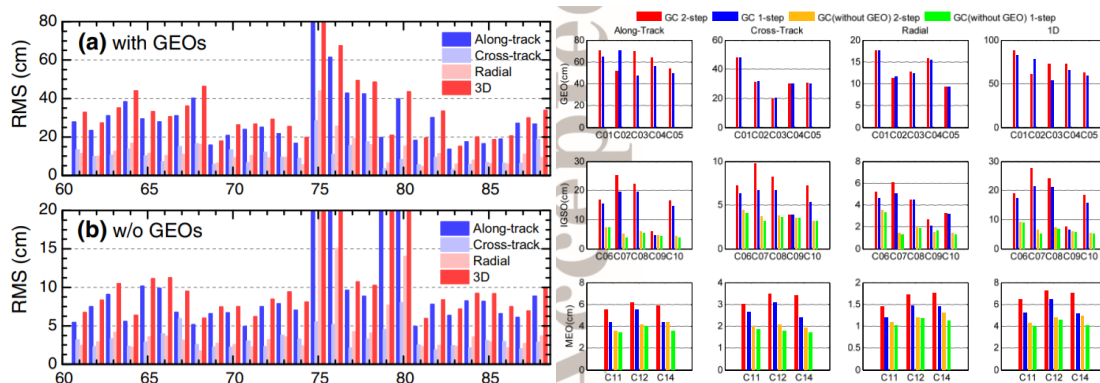


Fig. 1.8 POD results from Li (2017) and Li(2018)

To validate and evaluate the orbit accuracy of the BeiDou Navigation System (BDS), satellite laser ranging (SLR) data is used. The microwave-based precise orbits of BDS derived from four

Analysis Centers (ACs) are validated from 2013 to 2018, including three Multi-GNSS EXperiment (MGEX) ACs from WHU, CODE and GFZ, as well as a fourth AC, known as ISC in China, with the corresponding products designated as WUM, COM, GBM and ISC. The optimal SLR validated orbit accuracy of C01, C08, C10, C11 and C13 are 522.8 mm from WUM, 53.3 mm from ISC, 54.3 mm from ISC, 38.2 mm from ISC and 51.5 mm from COM, respectively. Due to the advantages of the orbit combination algorithm, the orbit accuracy of ISC is more stable and excellent for each of the validated BDS satellites (Yang, 2019; Qing, 2017; Peng, 2016). The dependency of SLR residuals is related with the satellite nadir angle. These correlations of SLR validation residuals are analyzed based on three types of BDS GEO, IGSO and MEO satellites (Fig. 1.9). The linear term means regression slope of SLR residuals as a function of the nadir angle (mm/degree).

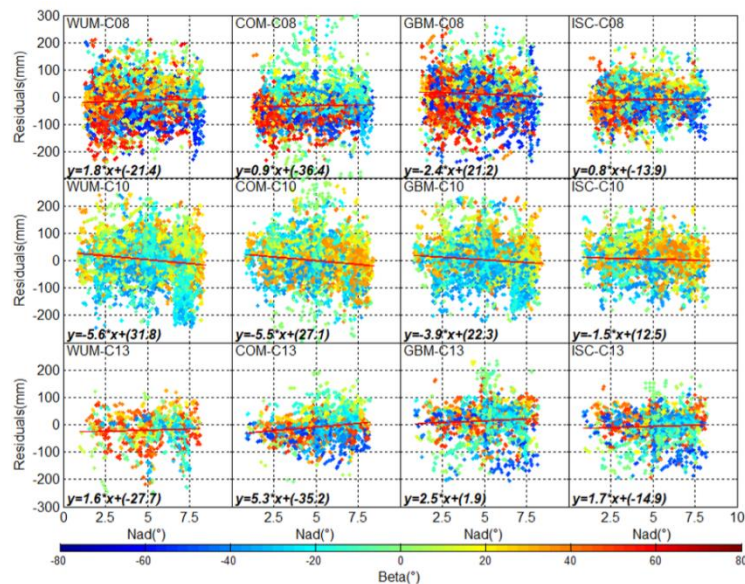


Fig. 1.9 The dependency of SLR residuals on the nadir angle

1.5.4 Positioning performance and improvement

With the development and improvement of GNSS, most topics of Precise Point Positioning (PPP) are becoming interesting (Chen, 2019; Liu, 2019; Li, 2018; Zhang, 2018; Li, 2019; Chen, 2016; Shi, 2017; Guo, 2016; Liu, 2017). In order to improve the PPP performance, inter-system bias and augmentation system are also developing (Li, 2018;).

Precise Point Positioning (PPP) technique enables stand-alone receivers to obtain cm-level positioning accuracy. Observations from multi-GNSS systems can augment users with improved positioning accuracy, reliability and availability. There are many researches about the multi-frequency PPP and multi-system combined PPP. To evaluate the performance of combined GPS/BDS PPP, the across-satellite single-difference (ASSD) GPS+BDS combined ambiguity-fixed PPP model is used, the percentage of fixing within 10 min for GPS only is 17.6%, when adding

IGSO and MEO of BDS, the percentage improves significantly to 42.8% in kinematic mode. The fixing percentage is 32.9% and 53.3% for Model GPS only and GPS+BDS in static mode (Liu, 2017). Kinematic and static combined GPS/BDS PPP positions are compared to the IGS daily estimates. The results indicate apparent improvement of GPS/BDS combined PPP solutions, where much smaller standard deviations are presented in the magnitude distribution of coordinates RMS statistics (Fig. 1.10). The combined PPP not only improve the positioning performance, but also shorten the convergence time.

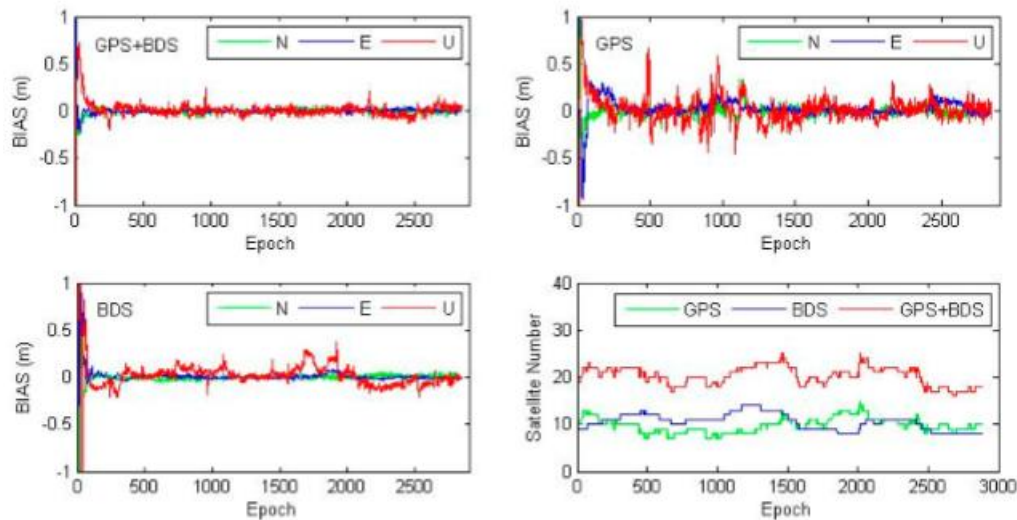


Fig. 1.10 GPS+BDS combined PPP

By adopting the real-time observations of IGS, multi-GNSS experiment (MGEX) and national BDS augmentation service system, BDS real-time wide-area PPP can be developed based on the high accuracy BDS real-time orbits, clocks and ionosphere products. This mode can provide centimeter-, decimeter- and meter-level positioning service with different positioning methods. The accuracy of dual-frequency PPP in high-latitude and western fringe region is about 0.2m and 0.3m in the horizontal and vertical component, respectively, while the horizontal accuracy is better than 0.1m and the vertical accuracy is better than 0.2m in the midlands, which is close to the accuracy of GPS real-time PPP. The flow chart is given in Fig. 1.11 At the same time, it is developed to be used in Android mobile terminal.

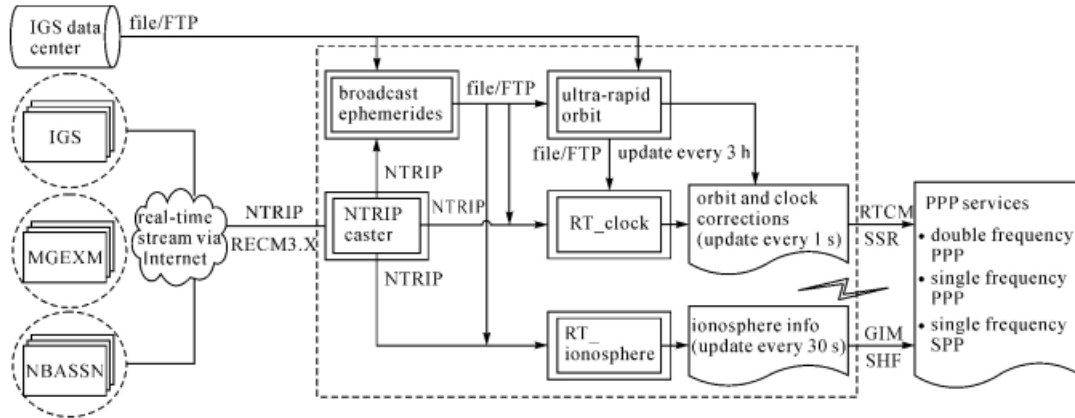


Fig. 1.11 Flow chart of BDS real-time PPP

The latest generation of GNSS satellites such as GPS BLOCK-IIIF, Galileo and BDS are transmitting signals on three or more frequencies, thus having more choices in practice. PPP tests with real triple-frequency data were performed in both static and kinematic scenarios. Results show that the three triple-frequency PPP models agree well with each other. Additional frequency has a marginal effect on the positioning accuracy in static PPP tests. However, the benefits of third frequency are significant in situations of where there is poor tracking and contaminated observations on frequencies B1 and B2 in kinematic PPP tests (Guo, 2016). Triple-frequency PPP has better positioning performance and less residuals compared to dual-frequency PPP (Fig. 1.12).

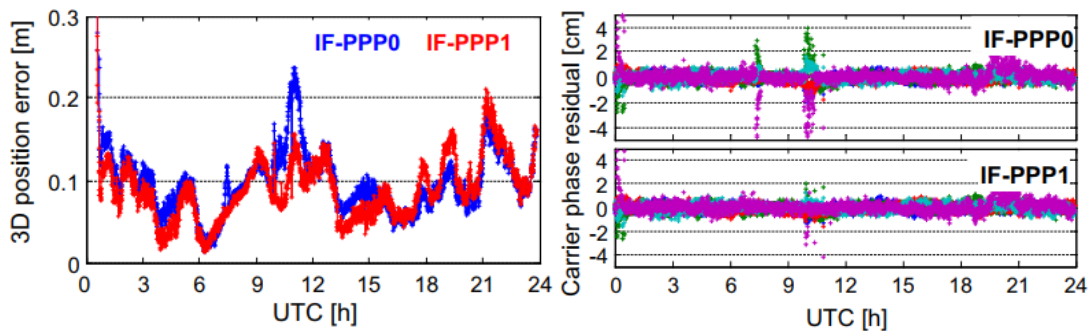


Fig. 1.12 3D positioning error and carrier phase residuals of triple-frequency PPP and dual-frequency PPP on JFNG station

Ambiguity resolution is the most important problem of PPP. Combined multi-system PPP has more complex uncalibrated phase delay (UPD). For UPD estimation, the GCRE-combined PPP solutions of the globally distributed MGEX and IGS stations are performed to obtain four-system float ambiguities and then UPDs of GCRE satellites can be precisely estimated from these ambiguities. Data recorded from 140 MGEX and IGS stations for a 30-day period in January in 2017 were used to validate the proposed GCRE UPD estimation and multi-GNSS dual-frequency PPP AR. GCRE four-system PPP AR enables the fastest time to first fix (TTFF) solutions and the highest accuracy for all three coordinate components compared to the single and dual system. Fig.

1.13 and Fig. 1.14 show that WL UPDs from CMONOC have better stabilities when the code biases are corrected with the improvements of 16.7, 27.6 and 85.9% for GEO, IGSO and MEO satellites, respectively.

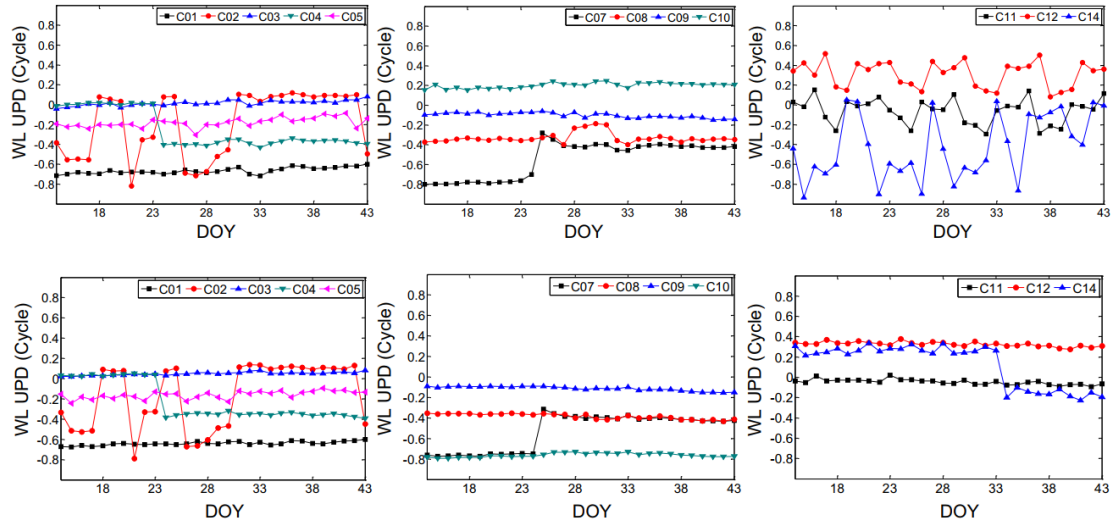


Fig. 1.13 BDS WL UPDs (The upper and bottom panels are for WL UPDs before and after the code bias correction, respectively.)

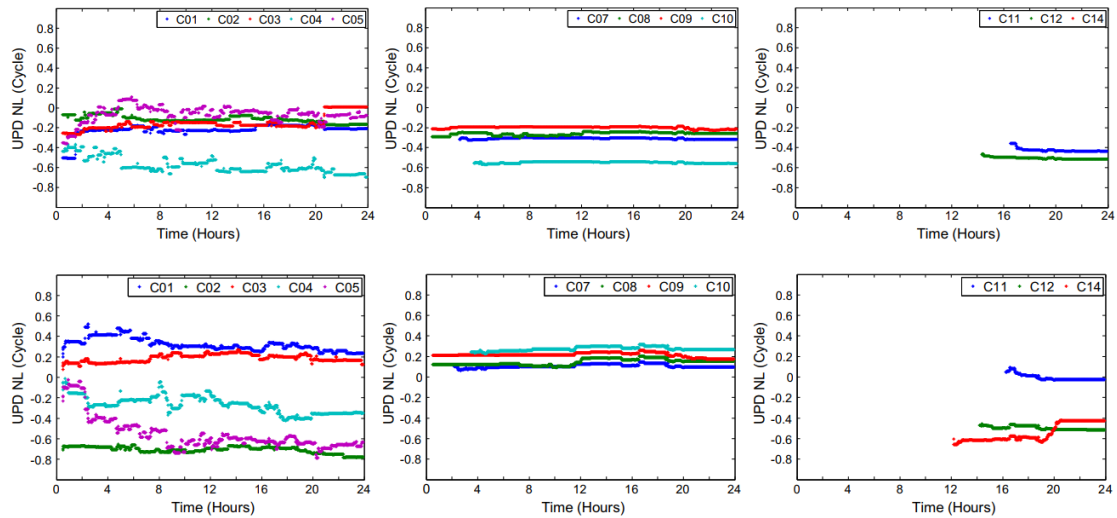


Fig. 1.14 BDS NL UPDs (The upper and bottom panels are for WL UPDs before and after the code bias correction, respectively.)

1.6 Development on the seafloor geodetic network

Funded by the national Key R&D Program of China, CASM (Chinese Academy of Surveying and Mapping) are undertaking the Marine Geodetic Datum and Navigation Techniques (2016YFB0501700) from 2016 to 2020, of which the project header is Prof. Yang Yuanxi who is one of the famous geodesists and navigation experts and the academicians of the Chinese Academy of Sciences.

For establishing the national seafloor geodetic network of China in the near future, the shallow sea and deep sea shelters equipped with sonar beacons and pressure gauges were developed by the National Deep Sea Center of China, one of the project participants. The shelters adopt new designs for long-term stable working located in the seafloor. The working frequency of the sonar sensor installed in the seafloor geodetic station is between 8kHz-16kHz, of which the working water depth can reach over 6000 meters and the relative ranging precision can reach 5/1000.

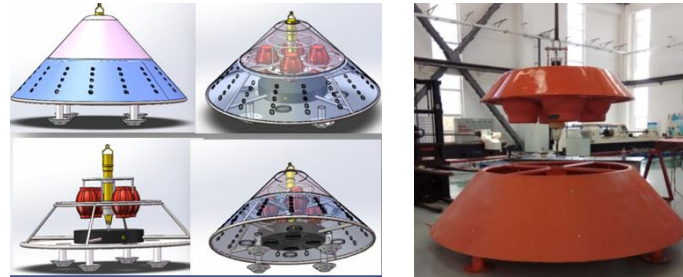


Fig. 1.15 Shallow sea sea shelter

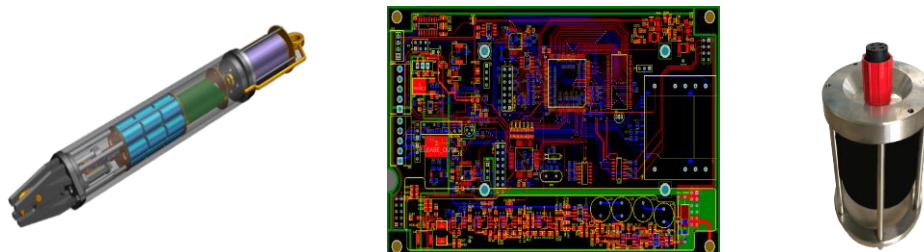


Fig. 1.16 The sonar beacon the key seafloor geodetic positioning equipment

During January and October, 2018, two test experiments are performed in shallow sea areas in the China Yellow Sea. It show that, the sonar positioning precision of the seafloor geodetic point is better than 0.1m.

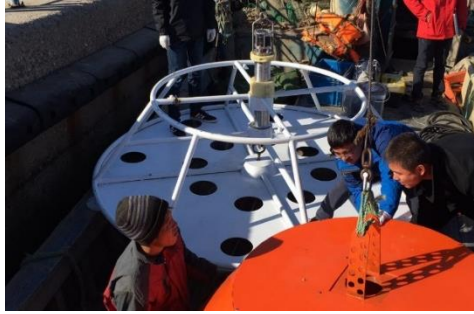


Fig. 1.17 The seafloor geodetic point deployment

In the past four years, there were a group of Chinese geodetic scholars, including Prof. Yang Yuanxi, Prof. Liu Yanxiong, Sun Dajun, Prof. Wang Zhenjie and Prof. Zhao Jianhu, Prof. Ly Zhiping, Prof. Xu Tianhe and etc., who contributed great efforts in this research area supported the national Key R&D project mentioned at the very beginning of this section.

In the past decades, China established the relatively complete geodetic datum covering the land areas, including the new developed China Geodetic Coordinate System 2000 (CGCS 2000) and the national gravity datum 2000. However, the currently used geodetic infrastructures have not well covered the sea areas of China. So, the marine geodetic datum and marine navigation technologies need to be further developed and extended to satisfy the national demands of marine security and developing marine economy in new era of China.

In 2017, a review and prospective study was made by Prof. Yang Yuanxi and his study group members by analyzing key technologies for establishing the national marine geodetic datum, current trends and future directions for developing the national marine geodetic datum and marine navigation technologies. In addition, Prof. Liu Jingnan, also as the academician of the Chinese Academy of Sciences, has discussed the development and trends of marine space-time frame network, that the marine space-time frame network still sees its construction in an initial stage and there is a universally great demand for global and national marine environment monitoring.

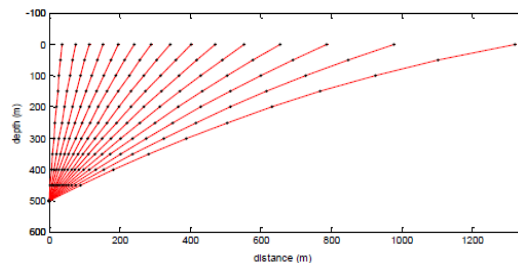


Fig. 1.18 Sonar ray blending characters relative to incidence angles

It is known that the estimation of atmospheric delay is an important part of the precise GNSS data analysis. In order to test the relationship between the accuracy of sound ray tracking and the

elevate angle, the project group take China Songhua Lake experiment as the test data.

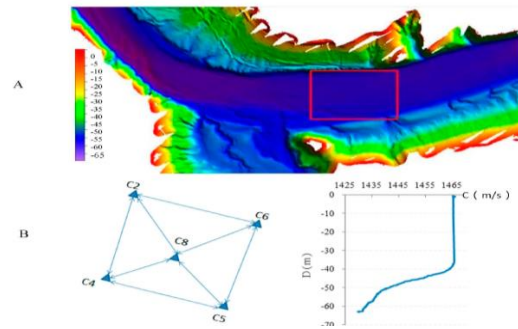
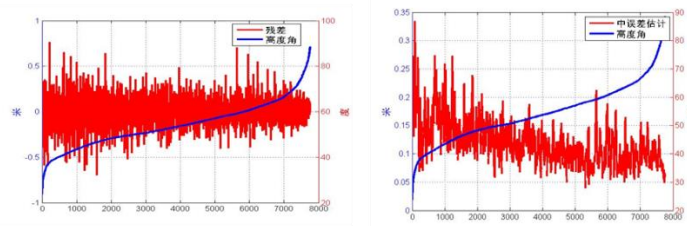


Fig. 1.19 Experiment in Songhua Lake



a. residual with increased elevate angle b. accuracy with increased elevate angle

Fig. 1.20 Residual and accuracy of ranging

In the latest two years, great efforts on improving the seafloor positioning precision were made, including the improvements on the sonar positioning function model and stochastic model. The representational works are from the study group headed by Prof. Wang Zhenjie as well as the group headed by Prof. Yang Fanlin.

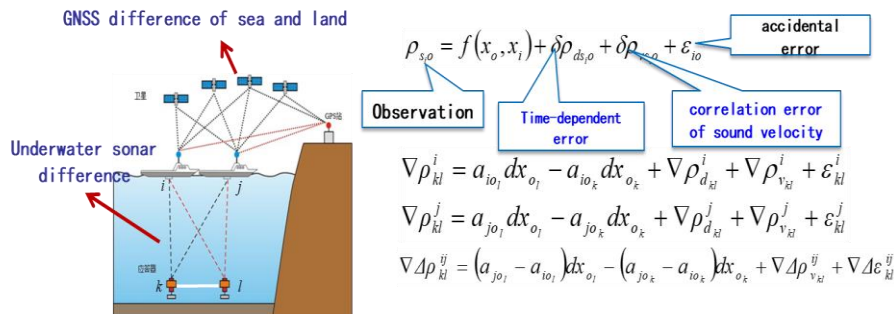


Fig. 1.21 Underwater Differential Positioning model

By using the sound ray tracking positioning model, the relationship between the residual size and the elevate angle was revealed. The result shows that, the variation of residual is obviously increased with the decreased elevate angle as shown in Fig. 1.20 Residual and accuracy of ranging.

Table 1.1 Sonar ray blending estimation model

No.	Compensate model	Author/data	Remarks
1	$a_0 + a_1(t_i - t_0)$	Fujita M, 2006	Linear regression
2	$a_0 + a_1(t_i - t_0) + a_2(t_i - t_0)^2$	Fujita M, 2006	Quadratic regression
3	$a(\tau_i - \tau_{\min} \sin \alpha)^2$	Yang FL et al 2011	Elevation related model
4	$w / \sin^3 \alpha + b$	Liu HM et al 2019	Elevation related model

As is well-known, in the past decade, Japanese scholars made great pioneering contributions on improving the sonar positioning models. These new studies from China may be as complementary new explorations for further improving the seafloor positioning precision. The new model is further developed and verified by the real experimental data, as shown the Fig. 1.18 and Table 1.2

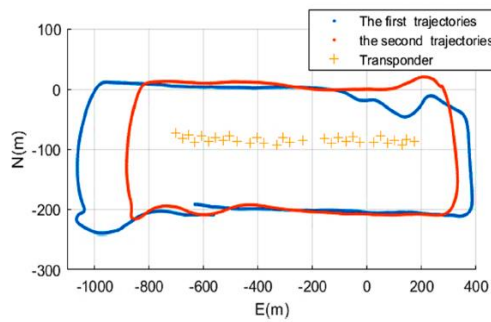


Fig. 1.22 Verification data from the China South Sea

Table 1.2 The new model verification Unit:m

Methods	LS1	LS2	Yang(201)2	Liu(2019)
Horizontal	0.52	0.51	0.56	0.30
Vertical	0.36	0.42	0.96	0.25

Bibliography

[1] CHENG Pengfei, CHENG Yingyan. The Current Status and Tendency of China Millimeter

- Coordinate Frame Implementation and Maintenance[J].Acta Geodaetica et Cartographica Sinica, 2017, 46(10):1327-1335.DOI:10.11947/j.AGCS.2017.20170336
- [2] Cheng Yingyan, Wang Hu, Xu Changhui, Zhang Yonghao, Xing Yunjian. Analysis on Application and Maintenance of Multi-technical Based global Reference Frame[J], Science of Surveying and Mapping, 2019 , 44(06):37-46.
- [3] CHENG Pengfei, CHENG Yingyan, An Overview of the CGCS2000 Coordinate Processing Technique Based on GNSS[J],Geomatics and Information Science of Wuhan University, 2018,43(12):2071-2078.
- [4] CHEN Jun-yong, YANG Yuan-xi, WANG Ming. Establishment of 2000 National Geodetic Control Network of China and It's Technological Progress. 2007,36(1):1-8
- [5] Cheng Peng-fei, Cheng Ying-yan, Mi Jin-zhong. CGCS2000 Plate Motion Model. Acta Geodaetica et Cartographica Sinica. 2013,42(2):159-167
- [6] Chen Junping, Wang Jungang,Zhang Yize,Yang Sainan,Chen Qian,Gong Xiuqiang. Modeling and Assessment of GPS/BDS Combined Precise Point Positioning.[J]. Sensors (Basel, Switzerland),2016,16(7).
- [7] Chen Jun-Yong. Thinking to improve and update the China geodetic coordinate system. 1999, 6(1): 2-4
- [8] Dang Ya-ming, Chen Jun-yong. GGOS and the new developments of geodesy. Science of Surveying and Mapping. 2006, 31(1): 131-133
- [9] Fei Guo,Xiaohong Zhang,Jinling Wang,Xiaodong Ren. Modeling and assessment of triple-frequency BDS precise point positioning[J]. Journal of Geodesy,2016,90(11).
- [10] Gu Guo-hua. Reference Frame, Coordinate Transformation and Crustal Movement. Bulletin of Surveying and Mapping. 2006, 8(1): 24-27
- [11] Honglei Yang,Tianhe Xu,Wenfeng Nie,Fan Gao,Meiqian Guan. SLR validation and evaluation on BDS precise orbits from 2013 to 2018[J]. Advances in Space Research,2019,64(2).
- [12] Jing Wei-ping, Li Zhao. Some Thoughts on Establishment and Maintenance of Terrestrial Reference Frame Considering Non-linear Variation. Geomatics and Information Science of Wuhan University. 2010, 35(6): 665-669
- [13] Jian Chen,Dongjie Yue,Shaolin Zhu,Hao Chen,Zhiqiang Liu,Xingwang Zhao. Correction model of BDS satellite-induced code bias and its impact on precise point positioning[J]. Advances in Space Research,2019,63(7).
- [14] Lu Zhi-ping, Wei Zi-qing. The Establishment of High Precise Coordinate Transformation Grid Model of CGCS2000. Acta Geodaetica et Cartographica Sinica. 2013,42(6):791-797
- [15] Liu Jing-nan, Liu Hui. Some Thoughts on the Establishment of Nationwide Continuously Operating Reference Stations. Geomatics and Information Science of Wuhan University. 2009,

34(11): 1261-1265

- [16] Liu Jing-nan, Yao Yi-bin, Shi Chuang. Method for Establishing the Speed Field Model of Crustal Movement in China. Geomatics and Information Science of Wuhan University. 2002, 27(4): 331-335
- [17] Li, Z Lu. et al. Parallel resolution of large-scale GNSS network un-difference ambiguity. Advance in Space Research,2017
- [18] Li M, He K et al, Robust adaptive filter for shipborne kinematic positioning and velocity determination during the Baltic Sea experiment, GPS Solutions, 2018, 22:81, DOI: 10.1007/s10291-018-0747-5 SCI, IF=4.727)
- [19] Liu Yuxi, Jia Xiaolin. Signal-In-Space precision analysis for IGSO and MEO satellites of BDS considering the age of data[J]. Journal of Geodesy and Geodynamics, 2018,38(04):390-393.
- [20] Li Jie, Zheng Zuoya, Zhang Dazhong, Li Dehai, Gu Shouzhou, Zhang Tao. Research on real-time BDS/GPS single-frequency PPP technology for Android mobile terminal[J]. Science of Surveying and Mapping, 2019,44(03):149-153.
- [21] Min Li,Wenwen Li,Chuang Shi,Kecai Jiang,Xiang Guo,Xiaolei Dai,Xiangguang Meng,Zhongdong Yang,Guanglin Yang,Mi Liao. Precise orbit determination of the Fengyun-3C satellite using onboard GPS and BDS observations[J]. Journal of Geodesy,2017,91(11).
- [22] Ma Xiaping, Lu Shangqiang, Li Qinzheng, Chen Peng. Evaluation of signal in space accuracy for BeiDou navigation satellite system[J].Science of Surveying and Mapping,2019,44(01):90-97.
- [23] Mingquan Lu,Wenyi Li,Zheng Yao,Xiaowei Cui. Overview of BDS III new signals[J]. Navigation,2019,66(1).
- [24] Peng Hanbing, Yang Yuanxi, Wang Gang, He Haibo. Performance Analysis of BDS Satellite Orbits during Eclipse Periods: Results of Satellite Laser Ranging Validation[J]. Acta Geodaetica et Cartographica Sinica,2016,45(06):639-645.
- [25] Qing Yun, Lou Yidong, Dai Xiaolei. Orbit Determination of BDS GEO and IGSO Satellites Using Combined GNSS and SLR Observations[J].Journal of Geodesy and Geodynamics, 2017,37(05):467-471.
- [26] Qi et al. Analytical optimization on GNSS buoy array for underwater positioning, Acta Oceanologica Sinica,2019
- [27] Shi Chuang, Zheng Fu, Lou Yidong. Research and evaluation of BDS real-time wide-area precise point positioning service system[J]. Acta Geodaetica et Cartographica Sinica, 2017, 46(10):1354-1363.
- [28] Wang Zhipeng,Shao Wei,Li Rui,Song Dan,Li Tinglin. Characteristics of BDS Signal-in-Space User Ranging Errors and Their Effect on Advanced Receiver Autonomous Integrity

- Monitoring Performance.[J]. *Sensors (Basel, Switzerland)*,2018,18(12).
- [29] Wei Zi-qing, Liu Guang-ming. China Geodetic Coordinate System 2000: Velocity Field in Mainland China. *Acta Geodaetica et Cartographica Sinica*. 2011,40(4):403-410
- [30] Wang Xiaoming, Cheng Yingyan, Wu Suqin, Zhang Kefei. An enhanced singular spectrum analysis method for constructing non-linear model of GPS site movement[J]. *Journal of Geophysical Research-Solid Earth*, 2016, 121(3):2193–2211.
- [31] Wang Xiaoming, Cheng Yingyan, Wu Suqin, Zhang Kefei. An effective toolkit for the interpolation and gross error detection of GPS time series[J]. *Survey Review*, 2016, 48(348):202-211.
- [32] Wei Zi-ping. National Geodetic Coordinate System:To Next Generation. *Geomatics and Information Science of Wuhan University*. 2003, 28(2): 138-143
- [33] Xin Xie, Rongxin Fang, Tao Geng, Guangxing Wang, Qile Zhao, Jingnan Liu. Characterization of GNSS signals tracked by the iGMAS network considering recent BDS-3 satellite[J]. *Remote Sensing*,2018,10:1736
- [34] Xingxing Li,Keke Zhang,Qian Zhang,Wei Zhang,Yongqiang Yuan,Xin Li. Integrated Orbit Determination of FengYun - 3C, BDS, and GPS Satellites[J]. *Journal of Geophysical Research: Solid Earth*,2018,123(9).
- [35] Xuexi Liu,Weiping Jiang,Zhao Li,Hua Chen,Wen Zhao. Comparison of convergence time and positioning accuracy among BDS, GPS and BDS/GPS precise point positioning with ambiguity resolution[J]. *Advances in Space Research*,2019,63(11).
- [36] Xingxing Li,Xin Li,Yongqiang Yuan,Keke Zhang,Xiaohong Zhang,Jens Wickert. Multi-GNSS phase delay estimation and PPP ambiguity resolution: GPS, BDS, GLONASS, Galileo[J]. *Journal of Geodesy*,2018,92(6).
- [37] Xin Li,Xingxing Li,Gege Liu,Guolong Feng,Fei Guo,Yongqiang Yuan,Keke Zhang. Spatial-temporal characteristic of BDS phase delays and PPP ambiguity resolution with GEO/IGSO/MEO satellites[J]. *GPS Solutions*,2018,22(4).
- [38] Xue S, Yang Y. Unbiased Nonlinear Least Squares Estimations of Short-distance Equations[J]. *The Journal of Navigation*, 2017, 70(4): 810-828.
- [39] Yang F et al. A TOA/AOA Underwater Acoustic Positioning System Based on the Equivalent Sound Speed, *Journal of Navigation*, 2018.
- [40] Yang Yuan-xi, Zha Ming, Song L, et al. Combined adjustment project of national astronomical geodetic networks and 2000' national GPS control network. *Progress In Natural Science*, 2005,15(5): 435-441
- [41] Yueling Cao,Xiaogong Hu,Jinping Chen,Lang Bian,Wei Wang,Rui Li,Xue Wang,Yongnan Rao,Xin Meng,Bin Wu. Initial analysis of the BDS satellite autonomous integrity monitoring

- capability[J]. GPS Solutions,2019,23(2).
- [42] Yanyan Liu,Shirong Ye,Weiwei Song,Yidong Lou,Dezhong Chen. Integrating GPS and BDS to shorten the initialization time for ambiguity-fixed PPP[J]. GPS Solutions,2017,21(2).
- [43] Zhang Xiaohong, Liu Gen, Guo Fei, Li Xin. Model comparison and performance analysis of triple-frequency BDS precise point positioning[J]. Geomatics and Information Science of Wuhan University, 2018,43(12):2124-2130.
- [44] Zhaoshuang et al., Investigation on underwater positioning stochastic model based on acoustic ray incidence angle ,Applied Ocean Research,2018.
- [45] Zhang B et al. Research on Acoustic Velocity Correction Algorithm in Underwater Acoustic Positioning[M], CSNC, 2018
- [46] Zhao J et al. Localization of an Underwater Control Network Based on Quasi-Stable. Sensors 2018, 18, 950.
- [47] Zhu Hua-tong. A Review of the Geodetic Reference System: Past, Present and Future. China Academic Journal Electronic Publishing House. 1989, 2(1):11-17

2. Earth gravity field and height datum

2.1 Earth gravity field

Yu et al. (2015) et al. proposed a recursion arithmetic formula for Legendre functions of ultra-high degree and order on every other degree. It can be acclaimed that the computation accuracies of Legendre functions up to complete degree and order 20000 can reach 10^{-10} at least if the recursion arithmetic on every other degree is applied. The recursion arithmetic on every other degree is suitable to compute Legendre functions of ultra-high degree and order. The arithmetic has two main advantages: it has enough accuracies and its run-time is also acceptable compared with IDR. In all, the recursion arithmetic on every other degree is an efficient approach to compute Legendre functions of ultra-high degree and order.

Zou et al. (2016) proposed the simultaneous solution for precise satellite orbit and earth gravity model. The numerical results show that the strategy on the realization of the simultaneous solution method is valid, and reveal its advantages distinctly. It is assumed that the key technologies of the simultaneous solution method have been solved, and an advance from the simulation stage to the real data analyzing is achieved. Finally, some prospects and future work are discussed to exert the potential ability of this method.

Zou et al. (2016) studied on the earth gravity modeling by GOCE in individual accelerometer mode. To overcome the so called polar gap problem, or the data loss in the polar regions and the caused deterioration on the low order spherical coefficients of the earth gravity model, the GRACE data in the same time span are combined with the variance component estimation method, and the model WHU-GRGO-SST is built complete to degree and order 100. It has the same accuracy as the EGM2008 and GGM05S compared to the 6169 GPS/leveling benchmarks in USA when truncated to the same degree. The analysis shows that the bias parameters of the GOCE accelerometers have significant drifts. The results demonstrate the superiority of the methods used in this article and provide a more strict foundation for the building of a combined static GRACE/GOCE satellite gravity model with high resolution and high accuracy, and the auxiliary products server for the calibration of the GOCE gradiometer and profound processing of satellite gravity gradients.

By taking errors of non-conservative acceleration and attitude observations into account, Chen et al. (2016) computed a new time series of monthly gravity field models complete to degree and order 60 covering the period Jan. 2003 to Dec. 2012 from the GRACE data. The derived GRACE solution (called Tongji-GRACE02) is compared in terms of geoid degree variances and temporal mass changes with the other GRACE solutions, namely CSR RL05, GFZ RL05a, and JPL RL05. The results show that (1) the global mass signals of Tongji-GRACE02 are generally consistent with

those of CSR RL05, GFZ RL05a, and JPL RL05; (2) compared to CSR RL05, the noise of Tongji-GRACE02 is reduced by about 21 % over ocean when only using 300 km Gaussian smoothing, and 60 % or more over deserts (Australia, Kalahari, Karakum and Thar) without using Gaussian smoothing and decorrelation filtering; and (3) for all examples, the noise reductions are more significant than signal reductions, no matter whether smoothing and filtering are applied or not.

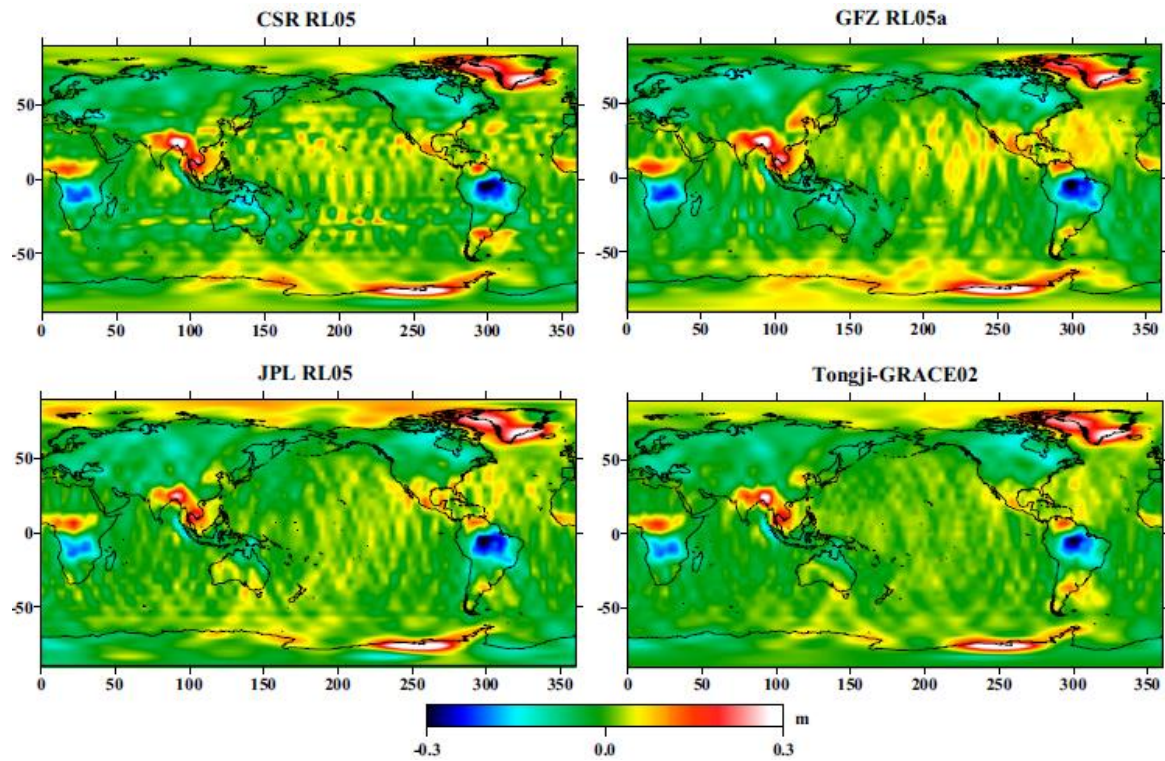


Fig. 2.1 Global mass variations (in EWH) derived from CSR RL05, GFZ RL05a, JPL RL05 and Tongji-GRACE02 of Oct. 2004 with a P4M6 decorrelation filtering and a 300-km Gaussian smoothing

Chen et al. (2016) established a modified dynamic approach for processing GRACE orbit and range-rate measurements, which treated orbit observations of the twin GRACE satellites as approximate values for linearization. Using the GRACE data spanning the period Jan. 2003 to Dec. 2010, containing satellite attitudes, orbits, range-rate, and non-conservative forces, they developed two global static gravity field models. One is the unconstrained solution called Tongji-Dyn01s complete to degree and order 180; the other one is the Tongji-Dyn01k model computed by using Kaula constraint. The comparisons between our models and those latest GRACE-only models (including the AIUB-GRACE03, the GGM05S, the ITSG-Grace2014k and the Tongji-GRACE01) published by different international groups, and the external validations with marine gravity anomalies from DTU13 product and height anomalies from GPS/levelling data, were performed in this study. The results demonstrate that the Tongji-Dyn01s has the same accuracy level with those of the latest GRACE-only models, while the Tongji-Dyn01k model is closer to the EIGEN6C2 than the other GRACE-only models as a whole.

He et al. (2016) selected 649 GPS leveling data distributed evenly over the mainland of China to compute the 1985 national height datum geopotential and the vertical discrepancy with respect to global vertical datum defined by EGM2008 using three methods. The final results demonstrate that the 1985 national height datum is 0.298 m and 0.4642 m above the mean sea level and the global geoid, respectively. Chen et al. (2017) refined the gravity field model by the Slepian localized spectral approach based on the scattered gravity data of Mainland China, and determined the gravity field variation model of Main China using the repeated gravity measurements from 2005 to 2008.

In Luo et al. (2016), a new monthly time-variable gravity field model WHU-Grace01s truncated to 60 degrees and orders is determined solely from GRACE KBRR data using dynamic integral approach. The accuracy of WHU-Grace01s has a good consistency with the previously published GRACE solutions. Shen (2017) proposed the methods for improving the accuracy of gravity recovery, which can be summarized as that refining the linearization method relative kinematic orbit to reduce the linearization error, modifying parameterization method to improve the property of observational equation and combined using analytic formula and numerical integration formula to increase the accuracy of orbit computation.

Lu et al. (2018) studied the IGGT (invariants of the gravitational gradient tensor) approach. A degree/order 240 gravity field model called IGGT_R1 is computed and its accuracy is evaluated by comparison with other gravity field models in terms of difference degree amplitudes, the geostrophic velocity in the Agulhas current area, gravity anomaly differences as well as by comparison to GNSS/leveling data.

Zhang et al. (2018) proposed a density interface modeling method using polyhedral representation to construct 3-D models of spherical or ellipsoidal interfaces such as the terrain surface of the Earth and applied to forward calculating gravity effect of topography and bathymetry for regional or global applications. The method utilizes triangular facets to fit undulation of the target interface. The model maintains almost equal accuracy and resolution at different locations of the globe. The method is applied to an area for the ellipsoidal Bouguer shell correction as an example and the result is compared to existing methods, which shows our method provides high accuracy and great computational efficiency.

For the downward continuation of gravity data, Huang et al (2018). proposed a point to point analytical model and a least-squares analytical model. In Liu et al. (2016), ultra-high-degree geopotential model, local topographic correction and remove-restore technique are suggested to be used for regard to the effect of topographic height, and for the realization of downward continuation combining with a transformation from spherical to undulating surface. Based on numerical analysis of the continuation models of traditional least squares method, improved least squares method and

Tikhonov regularization method, and according to the basic characteristics of spherical harmonic function, Liu et al (2018) proposed the improved Poisson integral iteration method.

Liang et al. (2018) computed an ultra-high gravity field model up to degree and order 2159 named SGG-UGM-1 using EGM2008 derived gravity anomaly and GOCE observation data. OpenMP technique is used for gravity modeling. SGG-UGM-1 derived height anomalies are validated by GPS leveling derived height anomalies in China and the standard deviation is 16.2 cm.

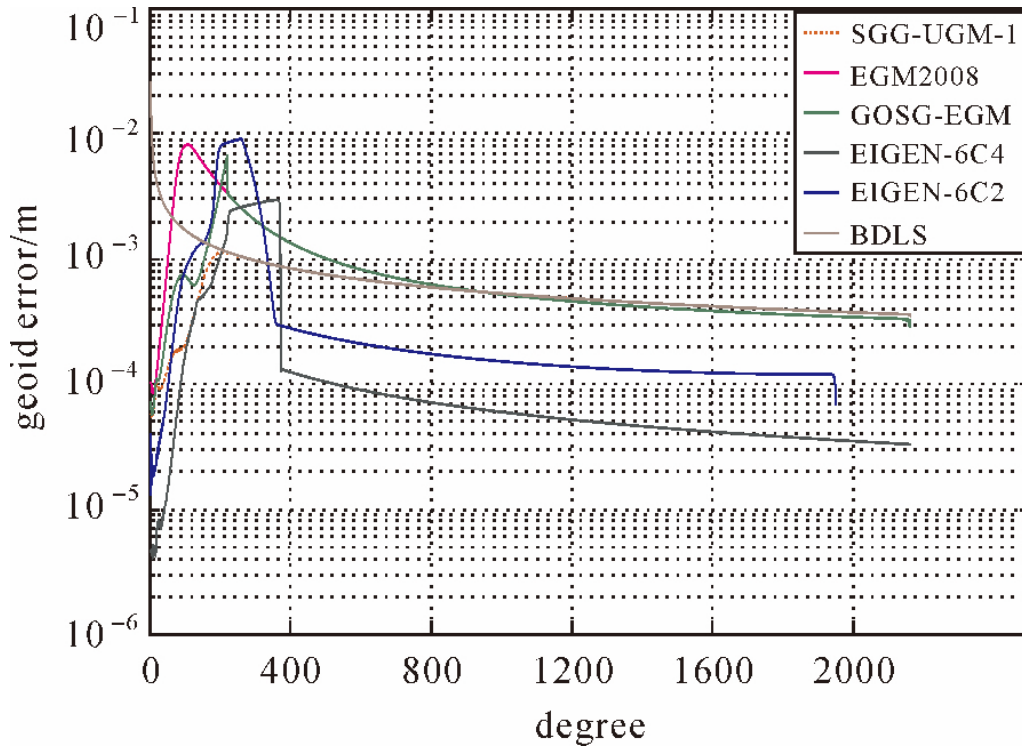


Fig. 2.2 Degree geoid error of the gravity field models

For fast computation of ultra-high-degree geopotential model by improved least-squares method, Tian et al. (2018) successfully reduced the matrix solution equation and designed the computation and storage method of Legendre function based on normal matrix block diagonalization using the increment characteristic of “secondary M” during the process of solving normal matrix by coefficient matrix solution method. The improved method compared to traditional block diagonal method can improve the efficiency by 300 times, by using this method one can solve ultra-high-degree geopotential model in ordinary PC, and the precision of the model has been improved by 5 orders of magnitude at least when compared with the numerical integral method.

In Huang et al. (2018), an evaluation system of survey accuracy targets including root mean square of errors(RMS),systematic error and mean error for marine and airborne gravity surveys is suggested. And an evaluation system of stability targets including calibration accuracy of scale value, total month zero drift, RMS of nonlinear month drift and limited deviation of nonlinear month drift is proposed. The methods of testing and evaluating the above technological targets are introduced.

And some key mathematic models about reduction of observed values for marine gravity survey, Eötvös correction for airborne gravimetry, platform tilt correction and evaluation of survey accuracy for air-sea-borne gravimetry are analyzed and modified. The obtained conclusions provide useful theoretical support for the revision of existing specifications for future civil-military inosculation of marine and airborne gravity surveys.

2.2 Height datum and geoid model

Li et al. computed an updated digital quasigeoid model (CNGG2011) for the national height datum 1985 of China by using Stokes-Helmert method. More than one million land gravity measurement, SRTM and 649 order B GPS/leveling data are used in the computation of CNGG2011. The average accuracy of CNGG2011 is 0.13 m in China, and 0.07 m and 0.14 m in eastern and western China, respectively. The average accuracy in each province is 0.06 m, and they are 0.05 m and 0.11 m in the East and the West of China respectively, and it is 0.22 m in the Tibet area. The relationship between the gravimetric geoid and the GPS/leveling data is also discussed and some strategies for geoid refinement in the future are also proposed for national height datum in China.

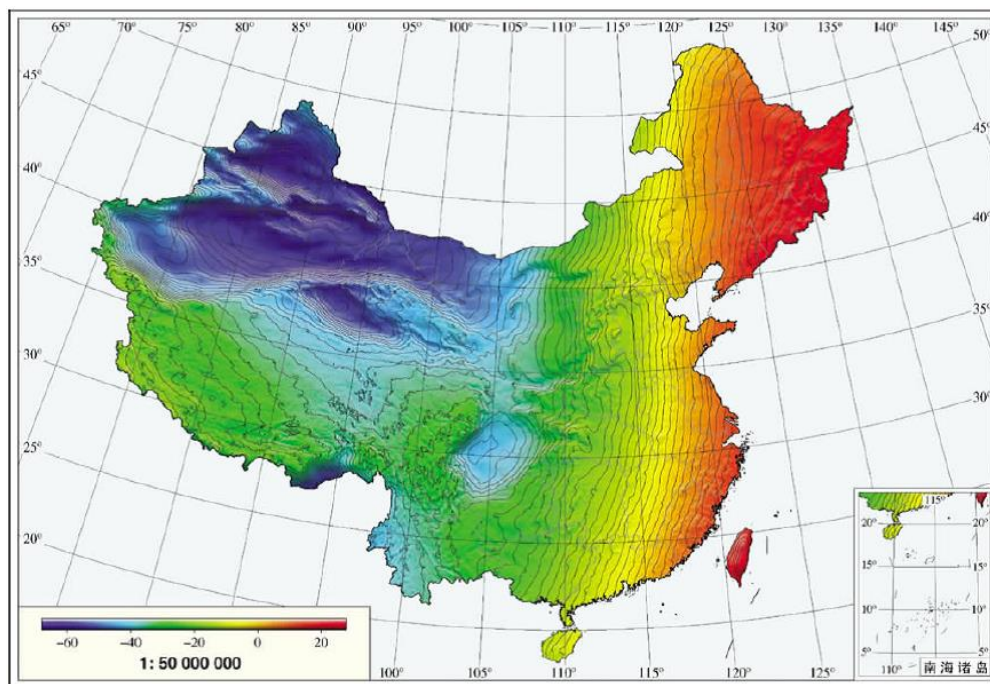


Fig. 2.3 The gravimetric quasigeoid (CNGG2011)

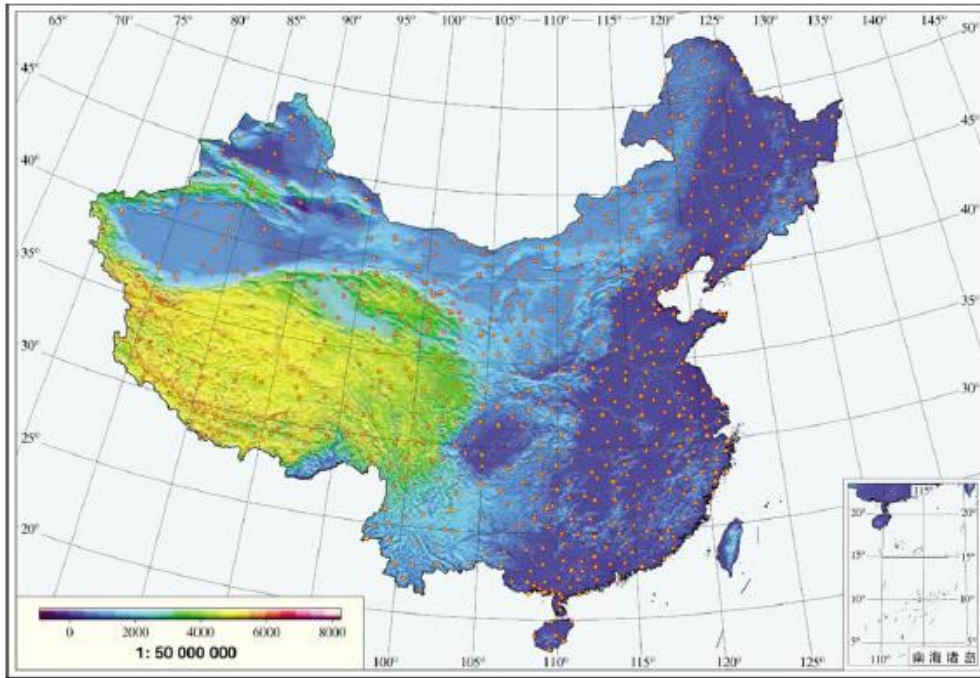


Fig. 2.4 GPS leveling data used for gravimetric quasi-geoid validation

Li et al. (2017) studied the vertical offset between China national height datum and global height datum. Based on potential difference approach and the height anomaly difference method, the vertical offset between the China 1985 national height datum and the global height datum corresponding to the normal gravity potential U_0 of GRS80, WGS-84 and CGCS2000 reference ellipsoidal from the 152 GPS/leveling points near the origin of Qingdao height origin and the EGM2008, EIGEN-6C4 and SGG-UGM-1 model. The regional datum is 23.1 cm lower than the global datum based on EIGEN-6C4 and WGS-84. When the Gauss-Listing geoid (mean sea surface) is selected as the global height datum, the China 1985 national height datum is 21.0 cm higher than the global height datum. The results also show that there are still large differences among the accuracies of the current gravity field models on these GPS/Levelling points around Qingdao, which will lead to big differences in estimating the vertical datum offset between the China 1985 national height datum and the global height datum with respect to different selected data sets.

Zhang et al. (2017) combined the land, altimetric, shipborne and airborne gravity data in the coastal area of mainland China by using an iterative procedure of the weighted least-squares prediction based on rectangular harmonic functions, and computed a coastal gravimetric quasigeoid model. The gravimetric quasigeoid model is compared with the height anomalies determined at 662 GPS leveling points over the coastal region of mainland China. The standard deviations of the differences in the coastal provinces range from 1.8 cm to 4.4 cm. For the entire computation area, the mean and standard deviation of the differences are 27.9 cm and 3.9 cm, respectively.

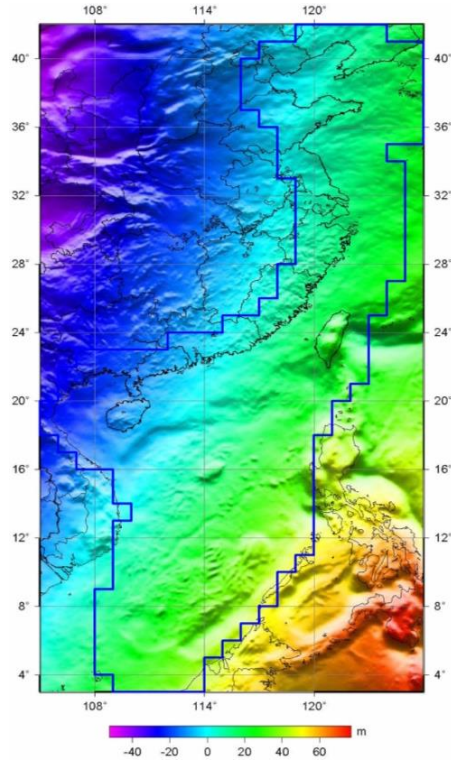


Fig. 2.5 2.5' \times 2.5' gravimetric quasigeoid model (m)

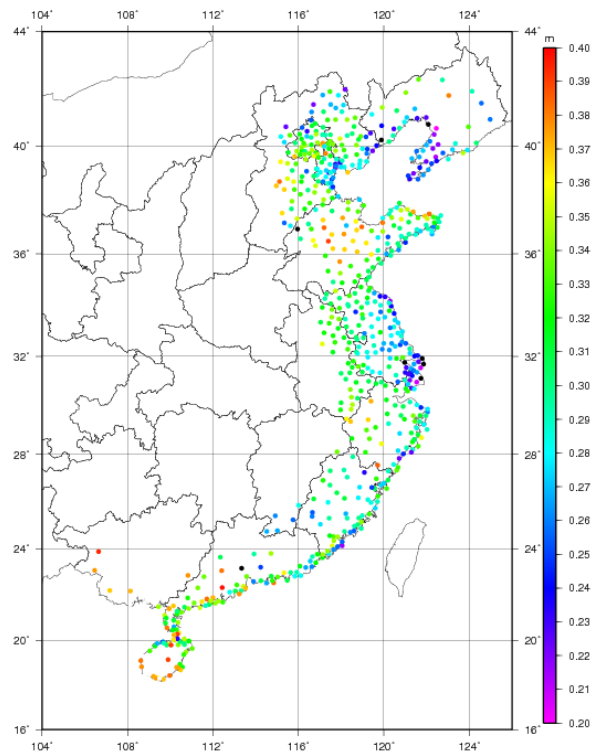


Fig. 2.6 Differences between GPS leveling derived height anomalies and the computed gravimetric quasigeoid (m)

Jiang et al. (2016, 2018) developed the spectral combination approach and propose a data-driven method for spectral weight determination of different gravity dataset. The spectral

combination for geoid computation is tested in southwest Texas area of USA and Mu Us area of China, respectively. For Texas case, the gravimetric geoid by combining GOCO03S, terrestrial (land and altimetric) gravity agrees with GSVS11 GPS/leveling data in ± 1.1 cm in terms of standard deviation. The addition of GRAV-D airborne gravity data collected at 11 km altitude improves the agreement to ± 0.8 cm over the 325 km traverse. For Mu Us case, the accuracy of the gravimetric quasigeoid model computed from the three data combination modes of GOCO05S & terrestrial gravity (5 km data spacing), GOCO05S & airborne gravity and GOCO05S & terrestrial (5 km data spacing) & airborne gravity are 0.8 cm, 1.8 cm and 0.8 cm, respectively.

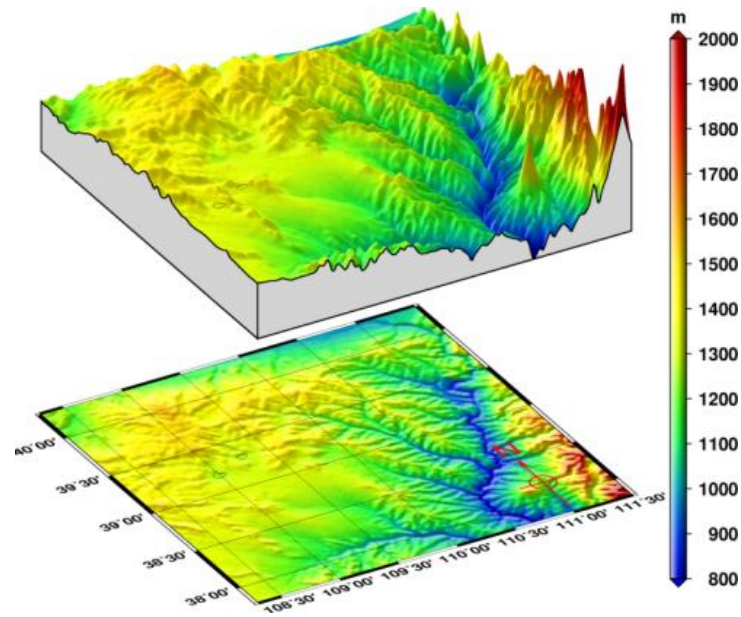


Fig. 2.7 Topography (right) of Mu Us area. Base map colors show the SRTM topography (m)

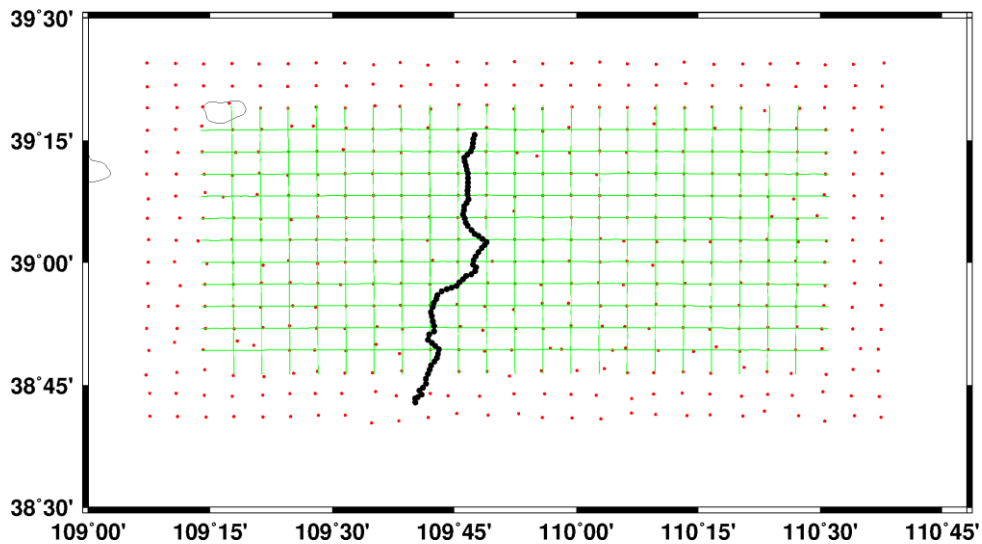


Fig. 2.8 Distribution of terrestrial (red), airborne (green) gravity and GPS leveling (black) data in Mu Us area

Table 2.1 Statistics of the differences between GPS leveling derived height anomalies and gravimetric quasigeoid models (Mu Us, m)

Terrestrial gravity point spacing	GOCO05S + Terrestrial				GOCO05S + Terrestrial + Airborne				Accuracy improvement
	Min	Max	Mean	Std	Min	Max	Mean	Std	
5 km	-0.310	-0.276	-0.299	0.008	-0.297	-0.246	-0.272	0.008	0%
10 km	-0.319	-0.279	-0.299	0.011	-0.301	-0.251	-0.272	0.010	9.1%
15 km	-0.348	-0.280	-0.307	0.015	-0.339	-0.254	-0.284	0.014	6.7%
20 km	-0.335	-0.253	-0.285	0.018	-0.340	-0.249	-0.280	0.016	11.1%
25 km	-0.389	-0.255	-0.303	0.033	-0.353	-0.247	-0.285	0.023	30.3%
30 km	-0.304	-0.212	-0.258	0.029	-0.332	-0.243	-0.274	0.015	48.3%

As a member of IAG JWG 2.2.2: The 1 cm geoid experiment, Tao Jiang (2018) applied the spectral combination approach and the SPECOM software in the Colorado geoid modeling experiment, a gravimetric geoid model was computed using terrestrial and airborne gravity data released by National Geodetic Survey of USA. The computed geoid model agrees with historic GPS leveling data in 5.3 cm in terms of standard deviation.

Moreover, the contributions of airborne gravity data in the data combination for geoid modeling were quantitatively evaluated in both Mu Us and Colorado geoid modeling experiment. It was found that for terrestrial gravity point spacing less than 15 km, airborne gravity data slightly improve the geoid accuracy by no more than 10% for both cases, and for terrestrial gravity point spacing larger than 15 km, the contributions of airborne gravity increase with the widening of the spacing of terrestrial data. The inclusions of airborne data improve the geoid accuracy by 11.1% - 48.3% for Mu Us case and 15.9% - 21.3% for Colorado case.

Wang et al. (2019) analyzed the elevation change of the national first order leveling point in recent years, it is concluded that the serious ground surface settlement occurred in some regions during the recent 20 years, The vertical crustal movement and local surface deformation are the major factors affecting the elevation changes, The first order leveling network should be monitored on a regular period which should be no more than 5 years and strives for 3 years. Base on the so-called 3D gravity vector method, Xing et al. (2018) computed a nationwide quasigeoid model by using gravity anomaly, vertical deflection, DEM and 6600 GPS leveling point data. It is reported in Xing et al. (2018) that the computed quasigeoid model agrees with 4241 GPS leveling derived height anomalies in 4 cm in terms of RMS.

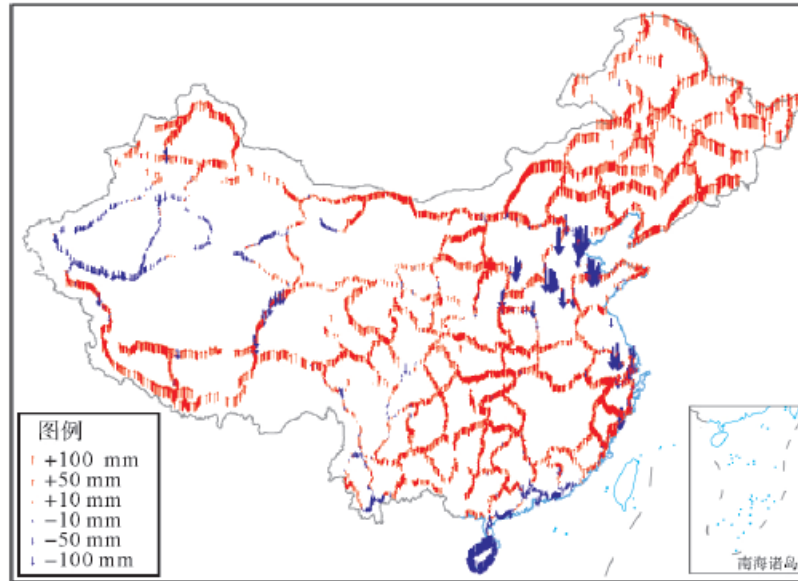


Fig. 2.9 Height changes observed by geodetic leveling network

2.3 Time variable gravity and related application

2.3.1 Post-processing method

Chen (2015) used synthetic data to simulate ice mass changes in the Amundsen Sea Embayment and Antarctic Peninsula, analyzed quantitatively the effects of a limited range of spherical harmonics coefficients and additional filtering, which in combination can significantly attenuate signal amplitudes. They presented details of a forward modeling algorithm and showed that it is capable of removing these biases from GRACE estimates.

Xu (2012) thought that the time varied Global gravity model provided by GRACE, there was system error in GRACE and the need for focusing on local areas, post-processing is required. In last decade, many algorithms have been shown to be effective, e.g. a Gaussian filter with isotropic and non-isotropic types, the destriping Filter, the empirical orthogonal functions method, wavelet analysis, and the Slepian function Method.

Zhang(2009) devised a new non-isotropic filter, called the fan filter: it is simply a 2-D double filter consisting of a low-pass along the degree n (the same as the conventional isotropic filter) simultaneously with a low-pass along the order m , whose contour projection onto the (n, m) plane is fan-shaped. It is deterministic and independent of a priori or external information, its implementation is straightforward, and the result is objective.

Huang (2019) estimated GWS anomalies in the highly karstic region (HKR) and low karstic region (LKR) in the Southwest China from GRACE TWS data. And they corrected the leakage errors in the estimated GWS anomalies through using the iterative forward modelling approach.

Li (2018) used a scale factor derived from the basin characteristic function to recover the attenuation signal. And proposed a so-called third-filter method to gain the temporal distribution of the leakage error.

Tang (2012) thought that errors exist in high degree and order spherical harmonics, which need to be processed before use. Filtering is one of the most commonly used techniques to smooth errors, yet it attenuates signals and also causes leakage of gravity signal into surrounding areas. They reported a new method to estimate the true mass change on the grid.

Mu (2017) proposed to use the Tikhonov regularization technique with the L-curve method to solve a correction equation which can reduce the leakage error caused by filter involved in GRACE data processing.

Jiang (2009) analyzed correlated errors exist in GRACE coefficients based on GRACE level-2 RL04 version time variable gravity data. The strategy of correlated error filter as determined and its effect was evaluated quantitatively by combining JASON-1 altimeter Data and WOA05 ocean model.

Cheng (2019) introduced the progress in applications of GRACE and Gravity field and steady-state ocean circulation explorer(GOCE)gravity satellite in the earth's gravity Field models and local mass change.

Qiujie (2018) used Tongji-Grace02s and Tongji-Grace02k data to study high-precision static GRACE-only global Earth's gravity field models derived by refined data processing strategies. Fan (2017) presented a state-of-the-art approach of passive-ocean Modified Radial Basis Functions (MBFs) that improves the recovery of time variable gravity fields from GRACE.

2.3.2 Terrestrial water storage variants monitoring

Wen (2016) used the independent component analysis(ICA)method to decompose the water storage changes derived from 132 months GRACE measurements. **Ni(2017)** investigated the ability of GRACE to quantitatively monitor long-term hydrological characteristics over the Lake Volta region. Principal component analysis (PCA) is employed to study temporal and spatial variability of long-term TWS changes.

Kao (2016) used GRACE gravity products from three data centers to determine sediment mass accumulation rates (MARs) and variability on the ECS inner shelf.

Yi (2016) adopted multiple remote sensing techniques to examine the diversified geophysical changes in the Tianshan; including glacier changes measured by GRACE and Ice, Cloud, and land Elevation Satellite (ICESat); lake level changes measured by radar altimetry; and snow coverage

measured by moderate-resolution imaging spectroradiometer (MODIS).

The considerable error sources mainly arise from the forward models that may be uncertain but indispensable to simulate some processes not directly measured or obtained by these observations. To minimize the use of these forward models, Gao(2019)estimated the mass change of ice sheet and present-day GIA using multi-geodetic observations, including GRACE and Ice, Cloud and land Elevation Satellite, as well as GPS, by an improved method of joint inversion estimate (JIE), which can solve simultaneously for the Antarctic GIA and ice mass trends.

Feng (2018) presented an overview of GWS changes in three main aquifers within China using GRACE data, and conduct a comprehensive accuracy assessment using in situ ground well observations and hydrological models. Monitoring areas include the North China Plain (NCP) (Feng et al., 2013), the Liaohe River Basin (LRB) (Zhong et al., 2018) , the Inner Tibetan Plateau. Zhong (2018) presented the trend of China land water storage redistribution at medi- and large-spatial scales in recent five years by satellite gravity observations.

Wu (2019) estimated GR using GRACE and GLDAS data. Gong (2018) collected data on GWS changes and land subsidence from in situ groundwater-level measurements, literature, and satellite observations to provide an overview of the evolution of the aquifer system during 1971-2015 with a focus on the sub-regional variations. Luo (2009) recovered the TWS variations in Heihe River basin based on a hybrid filtering scheme of the decorrelated filter P3M6 and 300km Gaussian filter, from GRACE Temporal gravity field models GRGS-EIGEN-GL04.

Tang (2017) developed a two-parameter annual water balance model for reconstructing annual terrestrial water storage change (DTWS) and groundwater storage change (DGWS). The model was integrated with the GRACE data and applied to the Punjab province in Pakistan for reconstructing DTWS and DGWS during 1980-2015 based on multiple input data sources.

Hao (2017) provided an overview of the development of drought monitoring and prediction systems (DMAPS) at regional and global scales. They highlighted advances in drought monitoring with multiple data sources and tools and prediction from multimodel ensemble.

2.3.3 Sea level change and Extreme climate monitoring

Chen (2018) analyzed global mean ocean mass change (GMOM) over the 12-year period (01/2005-12/2016) using three different GRACE RL05 monthly time-variable gravity solutions, and compare GRACE results with independent observations from satellite altimeter and Argo floats (i.e., Altimeter-Argo). Chen (2013) presented that the gap in the sea level budget disappears when combining gravity data from the GRACE satellite mission and temperature and salinity observations from the Argo programme collected between 2005 and 2011.

Cao (2015) used GRACE data for the quantitative investigation of the recent drought dynamic over the arid land of northwestern China, a region with scarce hydrological and meteorological observation datasets. Sun (2018) used GRACE satellite data to characterize and evaluate droughts and evaluated drought situations in the Yangtze River Basin (YRB) using the GRACE Texas CSR mascon (mass concentration) data from 2003 to 2015.

Yao (2016) investigated terrestrial water storage (TWS) changes over the Sichuan Basin and the related impacts of water variations in the adjacent basins from GRACE, in situ river level, and precipitation data and indicated that the Sichuan Basin TWS is shown to be influenced more by the Indian Ocean Dipole (IOD) than the El Niño-Southern Oscillation (ENSO).

Nie (2018) examined recent groundwater declines in the US High Plains Aquifer (HPA), a region that is heavily utilized for irrigation and that is also affected by episodic drought. To understand observed decline in groundwater and terrestrial water storage during a recent multi-year drought, and modified the Noah-MP LSM to include a groundwater irrigation scheme.

Zhou (2018) used multiple satellite remote sensing observations (e.g., GRACE, MODIS, Altimetry, and TRMM), hydrological models, and in situ data to characterize the flood phenomena over the Poyang Lake basin between 2003 and 2016. To improve the accuracy of the terrestrial water storage (TWS) estimates over the Poyang Lake basin, he introduced a modified forward-modeling method in the GRACE processing.

2.3.4 Load deformation motoring

Pan (2018) used the Empirical Orthogonal Function method characterize the spatial variations in the surface deformation with distinct seasonal oscillations at the GPS sites in five regions of the Tibetan Plateau. And found that these surface variations are highly correlated with the corresponding mass load signals observed by GRACE mission.

Chen (2018) thought that Global Positioning System observations in the Alps have now sufficient precision to reliably observe vertical surface movement rates. The geodynamic modeling of converging plate margins requires constraints on the origin of orogenic uplift, of which the two end members are pure crustal uplift and crustal thickening, respectively. He indicated that tectonic and hydrological signals superpose and cannot ignore the tectonic signal when using GRACE to invert for the equivalent water height (EWH).

Liu (2018) explored the seasonal and linear trend variations of surface vertical displacements caused by groundwater changes in NCP from 2009 to 2013 using GPS and GRACE techniques. Wang (2017) analysed 29 continuous GPS time series data together with data from GRACE to determine the seasonal displacements of surface loadings in the NCP. Results show significant

seasonal variations and a strong correlation between GPS and GRACE results in the vertical displacement component.

Zhang (2018) used 2.5 to 19-year-long time series from 35 CGPS stations to estimate vertical deformation rates in Nepal, which is located in the southern side of the Himalaya. GPS results were compared with GRACE observations. He conducted Principal to component analysis decompose the time series into three-dimensional principal components (PCs) and spatial eigenvectors.

Wang (2017) examined vertical load deformation at four continuous GPS sites in southern Greenland relative to GRACE predictions of vertical deformation over the period 2002–2016. With limited spatial resolution, GRACE predictions require adjustment before they can be compared with GPS height time series. Without adjustment, both GRACE spherical harmonic (SH) and mascon solutions predict significant vertical displacement rate differences relative to GPS. They used a scaling factor method to adjust GRACE results, based on a long-term mass rate model derived from GRACE measurements, glacial geography, and ice flow data.

Jia (2014) used the load Love numbers based on PREM (Preliminary Reference Earth Model) to the inversion of vertical load deformation on Earth's surface using GRACE. They thought the crustal structure under China mainland especially under Tibet Plateau was quite different from that given by PREM Earth model. They calculated new load Love numbers based on a modified Earth model which accounted for regional crustal structure in China mainland. And They investigated effect of regional crustal structure in China mainland for estimation of vertical load deformation on Earth's surface using GRACE RL05 data.

2.3.5 Low degree and geocenter motion study

Sun (2019) presented a new approach to estimate time variations in J2. Those variations are represented as a sum of contributions from individual sources. This approach uses solely GRACE data and the geoid fingerprints of mass redistributions that take place both at the surface and in the interior of the solid Earth. The results agree remarkably well with those based on satellite laser ranging, while estimates of the sources explain the observed variations in J2.

Zhang (2018) reconstructed the observed seasonal geocenter motion with geophysical model predictions of mass variations in the polar ice sheets, continental glaciers, terrestrial water storage (TWS), and atmosphere and dynamic ocean (AO). The reconstructed geocenter motion time series was shown to be in close agreement with the solution based on GRACE data supporting with an ocean bottom pressure model.

Chen (2005) estimated terrestrial water storage variations using time variable gravity changes observed by GRACE satellites during the first 2 years of the mission. And they examined how

treatment of low-degree gravitational changes and geocenter variations affect GRACE based estimates of basin-scale water storage changes, using independently derived low-degree harmonics from Earth rotation (EOP) and satellite laser ranging (SLR) observations.

Sun (2017) developed a methodology to estimate monthly variations in degree-1 and C_{20} coefficients by combining GRACE data with oceanic mass anomalies (combination approach). With respect to the method by Swenson et al., the proposed approach exploits noise covariance information of both input data sets and thus produces stochastically optimal solutions supplied with realistic error information. Numerical simulations show that the quality of degree-1 and -2 coefficients may be increased in this way by about 30 per cent in terms of RMS error.

Guo(2015) utilized GRACE data from January 2003 To December 2012 obtained from GFZ and CSR respectively to analyze changes of the Earth's low Degree gravity field, they used the Morlet wavelet analysis to determine the periods of time series to form the independent time series of variations C_{20} , C_{21} , C_{22} , C_{30} , C_{40} , S_{21} and S_{22} .

2.3.6 Effect factors analysis and geophysical interpretation

Bai (2018) indicated that hydrological model parameters are typically calibrated by observed streamflow data. This calibration strategy is questioned when the simulated hydrological variables of interest are not limited to streamflow. Well-performed streamflow simulations do not guarantee the reliable reproduction of other hydrological variables. One of the reasons is that hydrological model parameters are not reasonably identified. GRACE-derived total water storage change (TWSC) data provide an opportunity to constrain hydrological model parameterizations in combination with streamflow observations.

Chen (2017) adopted the Least Difference Combination (LDC) method to obtain some improved atmospheric, oceanic, and hydrological/crospheric angular momentum (AAM, OAM and HAM/CAM, respectively) functions and excitation functions (termed as the LDCgsm solutions). And they adopted various GRACE and Satellite Laser Ranging (SLR) geopotential data to correct the non-global mass conservation problem, while polar motion data are used as general constraints. The LDCgsm solutions can reveal not only periodic fluctuations but also secular trends in AAM, OAM and HAM/CAM, and are in better agreement with polar motion observations,

Chen (2017) developed a snow and glacier melt model for a distributed hydrological model (Coupled Routing and Excess Storage model, CREST) using the Upper Brahmaputra River (UBR) basin in the TP as a case study. And they used Satellite and ground-based precipitation and land surface temperature as model forcing.

Qiao (2019) estimated the lake water storage changes of 315 lakes during the period of 1976–

2013 through an empirical equation based on Shuttle Radar Topography Mission (SRTM) DEM (Digital Elevation Model) data and Landsat images.

Li (2018) proposed an index named the “Dam Influence Index” (DII) to assess the influence of the Three Gorges Dam (TGD) on hydrological drought in the Yangtze River Basin (YRB) in China.

Ni (2017) provided a comprehensive analysis of global connections between interannual TWS changes and El Nino Southern Oscillation (ENSO) events, using multiple sources of data, including GRACE measurements, land surface model (LSM) predictions and precipitation observations.

Chen (2017) investigated both TWS and GWS change in Jing-Jin-Ji from 1979 to the 2010s, based on the global land data assimilation system (GLDAS) and the Earth2Observe (E2O) outputs, and used a night light index as an index of urbanization.

Deng (2017) analyzed the influence of climate change on TWS in Central Asia over the past decade using the Gravity Recovery and Climate Experiment satellites and Climatic Research Unit datasets.

Evapotranspiration (ET) is a critical component of the water cycle, and it plays an important role in global water exchange and energy flow. Sun (2018) used GRACE gravity satellite data to simulate the annual actual water consumption from 2003 to 2014 and to analyze the temporal and spatial evolution of the regional precipitation and the actual ET. They also applied the newly developed rainwater utilization potential index (IRUP) to quantify the sustainability of the water balance in the Loess Plateau. Li (2018) developed an improved regional ET estimating approach based on the water balance equation, by using GRACE, daily precipitation, and discharge data.

Zeng (2018) reconciled the state-of-the-art observations and simulations of evapotranspiration (ET) temporal variability through a diagnostic framework composed of an observation-model-theory triplet. Chen (2018) used monthly ET estimations (2003-2015) from a water budget analysis using GRACE satellites terrestrial water storage solutions (GRACE-ET) and LSMs (model simulated ET (hereafter MOD-ET)) to quantify human-induced ET in the Songhua River Basin (SRB).

Xing (2018) presented as a nonlinear relationship constrained by physical limits, the Budyko framework serves as a powerful tool used to estimate the averaged E at long-term scale. Given the ability of GRACE in effectively simulating the Δ TWS at monthly scale, and developed a model to estimate E based on the Budyko framework with mean monthly parameter of multi-years, and applied to the estimation of E for the 24 selected catchments in different climatic regions across

China.

2.4 Satellite altimetry

2.4.1 Method

In the research of satellite altimeter calibration method, for the calibration and calibration of satellite altimetry observations, the method of comparing the observations of offshore stations near the satellite ground trajectory with those of satellite observations is often used to achieve the purpose of calibrating satellite altimetry data. Guan Bin et al. analyzed and compared the absolute calibration methods of satellite altimeter based on direct comparison, summarized and compared the advantages and disadvantages of different methods, and put forward some suggestions on the selection of calibration field construction methods in China; Based on the direct absolute calibration method of GPS buoy, the feasibility evaluation method of IGDR data for calibration calculation is designed, and the difference of calibration results between IGDR and GDR data is compared by using the data from four major calibration stations in the world, which verifies the feasibility of the prior calculation of calibration results through IGDR data; Yang Lei and others make use of the Qianli Yan Sea which is the first operational operation in China. The above calibration field gives the sea surface height measurement deviations of HY-2A, Jason-2, Jason-3, Saral, Sentinel-3A and other satellite altimeters at home and abroad. The reliability of Chinese calibration results is verified by comparing with foreign calibration fields. The accuracy of Jason-2 spaceborne microwave radiometer is analyzed by using China Coastal Operational GNSS Station. The results show that the coastal operational GNSS system can be a satellite-borne microwave radiometer. Calibration of wave radiometer provides important data support.

In the research of satellite altimetry high precision lifting method, Zhai Zhenhe and others put forward the idea of Double-satellite tandem flight operation mode according to the future development trend and development demand of ocean altimetry satellites, and obtained the distribution of satellite ground observation in different time. By selecting three inversion zones of different latitudes, using two inversion methods of gravity field, they carried out experiments, believing that multiple inversion methods are different. Joint processing of orbital and precise satellite altimetry data will further improve the accuracy of gravity field inversion to a certain extent; Men Huatao et al. considered the influence of many factors on echo simulation results, and discussed the optimal simulation method. The results show that the accuracy of echo simulation can be improved obviously after considering the actual reflectance and emission waveform of ground objects; Zhang Wenhao et al. established the echo model simulator by deducing the laser echo model, taking into account the temporal and spatial distribution of laser energy, surface profile and surface reflection. The existing waveform matching method without considering the effect of surface

reflectance is improved by the influence of emittance and other devices and target parameters, which can provide a solution for the acquisition of laser elevation control points under complex surface conditions; In order to improve the accuracy of inversion of gravity anomalies in the central area by inverse Vening-Meinesz formula, Li Houpu et al. expressed the vertical deviation of the central area of altimetry data in the form of biquadratic polynomial interpolation, deduced a precise formula for calculating the central area effect in the rectangular area which is more consistent with the actual data distribution, and analyzed the error between the derived formula and the traditional formula by using model data calculation. Based on the law that the elevation of laser footprint points is correlated with the actual terrain, a mathematical model for rough calibration of laser pointing angle is constructed by using the existing terrain data, which improves the accuracy of laser altimetry of ZY-3 02 satellite obviously, and verifies the rationality of error analysis of satellite laser altimetry and the validity of the mathematical model for correcting laser pointing angle by using the existing terrain data. It provides a reference for eliminating the gross errors of satellite laser altimetry, and supports the on-orbit calibration of satellite-borne laser altimetry outfield. Zhang Guo et al. carried out geometric calibration of the orbit of ZY-3 02 through terrain matching and using the method of laying laser targets on the ground, and improved the accuracy of the measurement in flat areas.

2.4.2 Data Processing

In the past three years, Chinese scholars have studied the data processing methods of satellite altimetry:

Considering the correlation between the high-frequency correction signals of adjacent sea surface height observations before and after satellite altimetry, Ke Baogui et al. proposed a technical method to determine the optimal Gauss low-pass filter radius of sea surface height, which provided a way to select the low-pass filter radius, and improved the feasibility of extending the sea surface height model determined by satellite altimetry data to offshore waters. Pan et al. proposed a collinear rank-deficit adjustment algorithm which combines the advantages of traditional collinear adjustment and robust estimation to eliminate the gross errors in the rank-deficit free network. Mao Song et al. compared Cryosat-2 and ICESat Altimetry in all lakes of the Qinghai-Tibet Plateau and Tianshan Mountains. As a result, there is a systematic deviation of up to tens of meters between them, and the re-tracking method is used to process Cryosat-2 first-class products to eliminate the deviation, and it is considered that Cryosat-2 SARIn second-class products can not be directly used for joint analysis of multi-source data; Li Guoyuan et al. take ICESat data as an example to determine the peaks by Gauss decomposition of odd and even inflection points. To solve the problem of low position efficiency, a full-waveform data Gauss decomposition algorithm based on automatic identification of wave crest is proposed. The decomposition efficiency and decomposition accuracy

are improved. Tian Shanchuan et al. found that the water level along the satellite trajectory of Hongze Lake is in the shape of "V" when using altimetry satellite to monitor the water level. The result of waveform redistribution algorithm is included in the data and commonly used waveform redistribution algorithm.

2.4.3 Applications

In the past three years, Chinese scholars have used satellite altimetry data to conduct extensive application research in polar research, earth gravity field construction, seabed topography inversion, ocean tides, and water level monitoring of rivers and lakes, and have achieved rich results.

Li Fei and others used Kriging interpolation method to interpolate CryoSat-2 altimetry data, and established an Antarctic ice sheet DEM with resolution of 1 km; filled the data gap with the contour data of Antarctic Digital Database (ADD), and established the Antarctic ice sheet DEM ; Zhou Chunxia and others took the Antarctic Academy 12 and Cooke2 subglacial lakes as examples, and used ICESat repetitive orbit algorithm to advance the activity of subglacial lakes. The monitoring was carried out, and the influence of different topographic and elevation changes on the elevation change of subglacial lakes in the monitoring model was discussed and analyzed . Taking part of the South China Sea as an example, Ke Bao et al. extracted sea level elevation data from CryoSat-2 data to determine the sea level high gradient and its residual gradient. The residual gradient grid was transformed into the residual component of vertical deviation by collocation method, and then the inverse Vening-Meinesz formula was used. The residual gravity anomaly is calculated by FFT method, and the gravity anomaly in the experimental sea area is obtained by removing the recovery method and fusing the ship-borne gravity survey data. The result is better than the existing gravity field model. Using satellite altimetry gravity anomaly data and ship bathymetric data, Yung Xiaohong et al. inverted the seabed topography in some areas of the North Pacific Ocean, and obtained the seabed topographic model with 1'x1' resolution. The non-linear term in the inversion relationship is analyzed, and the feasibility of the method of seabed topographic inversion based on satellite altimetry data is verified. Li Dawei et al. used ERS-2 and Envisat data to analyze the orthogonal response along the orbit, and obtained the harmonic constants of ocean tides in the China Sea and the Western Pacific Ocean, and compared with the tidal station data. The results show that the method is feasible except for the S2 and K1 partial tides. In addition, the solar synchronous orbit altimetry satellite can extract reliable and reasonably distributed tidal harmonic constants; Fu Yanguang et al. used TOPEX/Poseidon and Jason-1 altimetry data during synchronous observation to calculate the systematic deviation in the South China Sea, and generated a unified tidal time series based on the average sea surface of TOPEX/Poseidon altimeter. The harmonic constants of eight main tidal components were obtained by harmonic analysis and response analysis

of the original orbits and the orbiting orbits at normal points, respectively, and were compared with global models and experiments. Comparing the data of tidal stations, this paper analyzed the accuracy distribution characteristics of ocean tide model in South China Sea; Cai Yu used Jason-2 data to monitor the water level change of Taupo Lake, New Zealand, and further discussed the relationship between water level change and precipitation; Wen Jingchuan et al. proposed a data quality based on the unstable quality of satellite altimetry data in the lake and reservoir area. The method of extracting water level is evaluated and screened. Taking Hongze Lake as an example, the result shows that the method is superior to the traditional method. Wang Hong and others discussed the application of satellite altimetry data in water level monitoring in the middle reaches of the Yangtze River based on the monthly average water level data and Jason-2 data of Hankou Hydrological Station for many years, and considered that satellite altimetry data can supplement the shortage of water level monitoring station data. The encryption of water level data in scarce areas has very important practical significance. Based on the adjustment theory of satellite image regional network, Cao Ning et al. proposed for the first time that laser altimetry data assisted satellite stereo image for image geometry model refinement processing, combined with the great improvement of laser altimetry data accuracy in recent years and the characteristics of laser altimetry data of resource No.3 02 satellite. With theory, the accuracy of satellite stereo data mapping is improved effectively.

GNSS reflectometry is an effective supplement to satellite altimetry in monitoring lake or sea level changes. Ground-based GNSS-R altimetry uses L-band signals directly from GNSS satellites and GNSS signals reflected from the ground to determine surface features, such as sea surface height measurement, sea surface roughness feature extraction, surface humidity estimation, etc..

Bibliography

- [1] Bai, P., Liu, X., & Liu, C. (2018). Improving hydrological simulations by incorporating GRACE data for model calibration. *Journal of Hydrology*, 557, 291-304.
- [2] Cai Yu, Ke Changqing. Monitoring Water Level Changes of Taupo Lake in New Zealand Based on Jason-2 Altimeter Data[J]. *Water Resources and Power*, 2017(8):31-34.
- [3] Caijun Xu , Zheng G.(2016). Review of the Post-processing Methods on GRACE Time Varied Gravity Data. *Geomatics and Information Science of Wuhan University*.
- [4] Cao Ning, Zhou Ping, Wang Xia, et al. Laser altimetry data-aided satellite geometry model refined processing[J]. *Journal of Remote Sensing*, 2018, v.22(04):69-80.
- [5] Cao Yanping, Nan Zhuotong, Cheng Guodong. (2015).GRACE gravity satellite observations of terrestrial water storage changes for drought characterization in the arid land of northwestern China. *Remote Sensing*, 7(1),1021-1047.

- [6] Chaolong Yao, Zhicai Luo, Haihong Wang, et al. (2016). GRACE-Derived terrestrial water storage changes in the Inter-Basin region and its possible influencing Factors: A case study of the Sichuan Basin, China. *Remote Sensing*, 8(6), 444.
- [7] Chen Q, Shen Y, Chen W, et al. An improved GRACE monthly gravity field solution by modeling the non-conservative acceleration and attitude observation errors[J]. *Journal of Geodesy*, 2016, 90(6):503-523.
- [8] Chen Qiu jie, Shen Yunzhong, Zhang Xingfu, et al. GRACE Data-based High Accuracy Global Static Earth's Gravity Field Model[J] *Acta Geodaetica et Cartographica Sinica*, 2016,45(4):396-403. DOI:10.11947/j.AGCS.2016.20150422
- [9] CHEN Qiu jie, SHEN Yunzhong, ZHANG Xingfu, CHEN Wu, XU Houze. GRACE Data-based High Accuracy Global Static Earth's Gravity Field Model[J]. *Acta Geodaetica et Cartographica Sinica*, 2016, 45(4): 396-403.
- [10] Chen Shi, Xu Weimin, Wang Qianshen. The Spherical Harmonic Model of Gravity Field in Mainland China by Slepian Local Spectrum Method[J]. *Acta Geodaetica et Cartographica Sinica*, 2017,46(8):952-960. DOI:10.11947/j.AGCS.2017.20150542
- [11] Chen, H., Zhang, W., & Jafari Shalamzari, M. (2018). Remote detection of human-induced evapotranspiration in a regional system experiencing increased anthropogenic demands and extreme climatic variability. *International Journal of Remote Sensing*, 1-22.
- [12] Chen, J. L., Rodell, M., Wilson, C. R., et al. (2005). Low degree spherical harmonic influences on Gravity Recovery and Climate Experiment (GRACE) water storage estimates. *Geophysical Research Letters*, 32(14).
- [13] Chen, J. L., Wilson, C. R., & Tapley, B. D. (2013). Contribution of ice sheet and mountain glacier melt to recent sea level rise. *Nature Geoscience*, 6(7), 549-552.
- [14] Chen, J. L., Wilson, C. R., Li, J., et al. (2015). Reducing leakage error in GRACE-observed long-term ice mass change: a case study in West Antarctica. *Journal of Geodesy*, 89(9), 925–940.
- [15] Chen, J., Tapley, B., Save, H., et al. (2018). Quantification of ocean mass change using GRACE gravity, satellite altimeter and Argo floats observations. *Journal of Geophysical Research: Solid Earth*.
- [16] Chen, W., Braitenberg, C., & Serpelloni, E. (2018). Interference of tectonic signals in subsurface hydrologic monitoring through gravity and GPS due to mountain building. *Global and Planetary Change*, 167, 148-159.
- [17] Chen, W., Li, J., Ray, J., & Cheng, M. (2017). Improved geophysical excitations constrained by polar motion observations and GRACE/SLR time-dependent gravity. *Geodesy and Geodynamics*, 8(6), 377-388.

- [18] Chen, X., Long, D., Hong, Y., et al. (2017). Improved modeling of snow and glacier melting by a progressive two-stage calibration strategy with GRACE and multisource data: How snow and glacier meltwater contributes to the runoff of the Upper Brahmaputra River basin? *Water Resources Research*, 53(3), 2431-2466.
- [19] Chen, Z., Jiang, W., Wang, W., et al. (2017). The Impact of Precipitation Deficit and Urbanization on Variations in Water Storage in the Beijing-Tianjin-Hebei Urban Agglomeration. *Remote Sensing*, 10(2), 4.
- [20] Cheng Pengfei, Wen Hanjiang, Liu Huanling, et al. (2019). Research situation and future Development of satellite geodesy. *Geomatics and Information Science of Wuhan University*, 44(1): 48-54.
- [21] Cheng Pengfei, Wen Hanjiang, Liu Huanling, et al. Research progress in satellite gravity and satellite altimetry[J], *Science of Surveying and Mapping*, 2019,44(06),16-22.
- [22] Cheng Pengfei, Wen Hanjiang, Liu Huanling, et al. Research progress in satellite gravity and satellite altimetry[J], *Science of Surveying and Mapping*, 2019,44(06),16-22.
- [23] Chuanyin Zhang, Yamin Dang, Tao Jiang, Chunxi Guo, Baogui Ke & Bin Wang (2017): Heterogeneous Gravity Data Fusion and Gravimetric Quasigeoid Computation in the Coastal Area of China. *Marine Geodesy*, VOL. 40, NOS. 2–3, 142–159, DOI: 10.1080/01490419.2017.1282899
- [24] Deng, H., & Chen, Y. (2017). Influences of recent climate change and human activities on water storage variations in Central Asia. *Journal of Hydrology*, 544, 46-57.
- [25] Fan Y, Kusche J, Forootan E, et al. (2017). Passive - ocean radial basis function approach to improve temporal gravity recovery from GRACE observations[J]. *Journal of Geophysical Research Solid Earth*, 122(8).
- [26] Feng W, Shum C, Zhong M, et al.(2018). Groundwater Storage Changes in China from Satellite Gravity: An Overview. *Remote Sensing*, 10(5).
- [27] Feng, W., Zhong, M., Lemoine, J.-M., et al. (2013). Evaluation of groundwater depletion in North China using the Gravity Recovery and Climate Experiment (GRACE) data and ground-based measurements. *Water Resources Research*, 49(4), 2110-2118.
- [28] Fu Yanguang, Zhou Xinghua, Xu Jun, et al. Extraction of Tidal Information in the South China Sea Based on TOPEX/Poseidon and Jason-1 Altimeter Data[J]. *Geomatics and Information Science of Wuhan University*, 2018, 43(6):901-907.
- [29] Gao, Chunchun, Yang Lu, Zizhan Zhang, Hongling Shi, (2019). A Joint Inversion Estimate of Antarctic Ice Sheet Mass Balance Using Multi-Geodetic Data Sets, *Remote Sens*, 11(6).
- [30] Gong, H., Pan, Y., Zheng, L., et al. (2018). Long-term groundwater storage changes and land subsidence development in the North China Plain(1971-2015). *Hydrogeology Journal*, 26(5),

1417-1427.

- [31] Guan Bin, Sun Zhongmiao, Liu Xiaogang, et al. Feasibility of Calibration Computing Using IGDR Preliminarily[J]. *Hydrographic Surveying and Charting*, 2018,38(01),10-13+22
- [32] Guan Bin, Sun Zhongmiao, Liu Xiaogang, et al. Direct absolute calibration methods of satellite altimeter and its newest application[J]. *Progress in Geophysics*, 2017, 32(6):2326-2330.
- [33] Hao, Z., Yuan, X., Xia, Y., et al. (2017). An Overview of Drought Monitoring and Prediction Systems at Regional and Global Scales. *Bulletin of the American Meteorological Society*, 98(9), 1879-1896.
- [34] HUANG Motao, LIU Min, WU Taiqi, LU Xiuping, DENG Kailiang, ZHAI Guojun, OUYANG Yongzhong, CHEN Xin. Research and Evaluation on Key Technological Target System for Marine and Airborne Gravity Surveys[J]. *Acta Geodaetica et Cartographica Sinica*, 2018, 47(11): 1537-1548.
- [35] Huang, Z., Yeh, P. J.-F., Pan, Y., et al. (2019). Detection of large-scale groundwater storage variability over the karstic regions in Southwest China. *Journal of Hydrology*, 569, 409-422.
- [36] Jialei T, Xinxing L I, Xiaoping W U, et al. Fast Realization of Ultra-high-degree Geopotential Model by Improved Least-squares Method[J]. *Acta Geodaetica et Cartographica Sinica*, 2018,47(11):1437-1445.DOI:10.11947/j.AGCS.2018.20170659.
- [37] Jiang T (2018). On the contribution of airborne gravity data to gravimetric quasigeoid modelling: a case study over Mu Us area, China. *Geophysical Journal International*, Volume 215, Number 2, Page 1308, DOI: 10.1093/gji/ggy346
- [38] Jiang T , Wang Y M . On the spectral combination of satellite gravity model, terrestrial and airborne gravity data for local gravimetric geoid computation[J]. *Journal of Geodesy*, 2016, 90(12):1405-1418.
- [39] Jin-Yun G, Xue-Min Y U, Qiao-Li K, et al. Analysis of low degree gravity changes from GRACE gravity field model. *Progress in Geophysics*, 2015.
- [40] Kao, R. Wu, C.-R. Shih, H.-C. (2016). Sediment-Mass Accumulation Rate and Variability in the East China Sea Detected by GRACE. *Remote Sens.* 8, 777.
- [41] Ke Baogui, Xu Jun, Yang Lei, et al. Optimal Gaussian Low Pass Filtering Radius Selection for Determining Offshore Sea Surface Height with Jason-2 Data[J]. *Geomatics and Information Science of Wuhan University*, , 43(9):1309-1314.
- [42] Ke Baogui, Zhang Liming, Wang Wei, et al. Method of Construction Gravity Anomaly in Coastal Region of China Using Cryosat2 Altimetric and Shipborne Data[J]. *Journal of Tongji University (natural science)* , 2017(45):1531-1538.
- [43] Li Dawei, Li Jiancheng, Jin Taoyong. Research on Ocean Tides Derived from Sun-Synchronous Satellite Altimeter Data[J]. *Journal of Geodesy and Geodynamics*, 2018(1):24-

27.

- [44] Li Fei, Xiao Feng, Zhang Shengkai, et al. DEM Development and Precision Analysis for Antarcticice Sheet Using CryoSat-2 Altimeter Data[J].Chinese Journal of Geophysics, 2017(60):1617-1629.
- [45] Li GuoYuan, Cui Chengling, Chen Jiyi, et al. An improved method of Gaussian decomposition of satellite laser altimeter full waveform data[J]. Science of Surveying and Mapping, 2018, 43(10):121-128.
- [46] Li Guoyuan. Earth Observing Satellite Laser Altimeter Data Processing Method and Engineer Practice[J], Acta Geodaetica et Cartographica Sinica, 2018, 47(12):133.
- [47] Li Houpu, Bian Shaofeng, Ji Bing, et al. Precise Calculation of Innermost Area Effects in Altimetry Gravity Based on the Inverse Vening-Meinesz Formula[J]. Geomatics and Information Science of Wuhan University, 2019(2):200-205.
- [48] LI Jiancheng, CHU Yonghai, XU Xinyu. Determination of Vertical Datum Offset between the Regional and the Global Height Datum[J]. Acta Geodaetica et Cartographica Sinica, 2017, 46(10): 1262-1273.
- [49] Li Jiancheng. The recent Chinese terrestrial digital height datum model: Gravimetric Quasi-Geoid CNGG2011. Acta Geodaetica et Cartographica Sinica, 2012, 41 (5): 651-660, 669.
- [50] Li, F., Wang, Z., Chao, N., & Song, Q. (2018). Assessing the Influence of the Three Gorges Dam on Hydrological Drought Using GRACE Data. *Water*, 10(5), 669.
- [51] Li, Q., Luo, Z., Zhong, B., et al. (2018). An Improved Approach for Evapotranspiration Estimation Using Water Balance Equation: Case Study of Yangtze River Basin. *Water*, 10(6), 812.
- [52] Li, W., Zhang, C., Wen, H., et al. (2018). The effects of leakage error on terrestrial water storage variations in the Yangtze River Basin measured by GRACE. *Journal of Applied Geophysics*.
- [53] Liang Wei, Xu Xinyu, Li Jiancheng, et al. The Determination of an Ultra-high Gravity Field Model SGG-UGM-1 by Combining EGM2008 Gravity Anomaly and GOCE Observation Data[J]. Acta Geodaetica et Cartographica Sinica, 2018, 47(4):425-434. DOI:10.11947/J.AGCS.2018.20170269
- [54] Liu M, Huang M, Ouyang Y, et al. Test and Analysis of Downward Continuation Models for Airborne Gravity Data with Regard to the Effect of Topographic Height[J]. Acta Geodaetica Et Cartographica Sinica, 2016, 45(5):521-530 and 551.
- [55] Liu Xiaogang, Sun Zhongmiao, Guan Bin, et al. Downward Continuation of Airborne Gravimetry Data Based on Improved Poisson Integral Iteration Method[J]. Acta Geodaetica Et Cartographica Sinica, 2018, 47(9):1188-1195. DOI:10.11947/j.AGCS.2018.20170569.
- [56] Liu, R., Zou, R., Li, J., Zhang, C., et al. (2018). Vertical Displacements Driven by Groundwater

- Storage Changes in the North China Plain Detected by GPS Observations. *Remote Sensing*, 10(2), 259.
- [57] Lu B, Luo Z, Bo Z, et al. The gravity field model IGGT_R1 based on the second invariant of the GOCE gravitational gradient tensor[J]. *Journal of Geodesy*, 2017(4–5):1-12.
- [58] Lulu J, Longwei X, Hansheng W. (2014). Effects of Crustal Structure for Estimation of Vertical Load Deformation on the Solid Earth Using GRACE in China Mainland. *Advances in Earth Science*, 29(7):828-834.
- [59] Luo Z C, Li Q, Wang H H, et al. (2009). Terrestrial Water Storage Variations in the Heihe River Basin Recovered by GRACE Time-Variable Earth Gravity Field. *Egu General Assembly Conference*.
- [60] Luo Z C, Zhou H, Qiong L I, et al. A new time-variable gravity field model recovered by dynamic integral approach on the basis of GRACE KBRR data alone[J]. *Chinese Journal of Geophysics*, 2016,59(6):1994-2005,DOI:10.6038/cjg20160606.
- [61] Mao Song, Shen Qiang, Wang Hanming, et al. Bias Analysis of CryoSat-2 Level 2 Products in SARIn Mode over Inland Water[J]. *Journal of Geodesy and Geodynamics*,2019(5):482-486.
- [62] Men Huatao, Li Guoyuan, Chen Jiyi, et al. Refined Simulation Methods of Laser Altimetry Satellite Echo Waveform[J].*Chinese Journal of Lasers*, 2019, 46(01):310-317.
- [63] Miao Sun., Qin'ge Dong. Estimation of Actual Evapotranspiration in a Semiarid Region Based on GRACE Gravity Satellite Data-A Case Study in Loess Plateau. *Remote Sens. Inf.* 10(12), 2032. (In Chinese).
- [64] Motao H, Min L, Kailiang D, et al. Analytical solution of downward continuation for airborne gravimetry based on upward continuation method[J]. *Chinese Journal of Geophysics*,2018,61(12):4746-4757,DOI:10.6038/cjg2018L0594
- [65] Mu, D., Yan, H., Feng, W., et al. (2017). GRACE leakage error correction with regularization technique: Case studies in Greenland and Antarctica. *Geophysical Journal International*, ggw494.
- [66] Ni, S., Chen, J., Wilson, C. R., et al. (2017). Global Terrestrial Water Storage Changes and Connections to ENSO Events. *Surveys in Geophysics*, 39(1), 1–22.
- [67] Nie, W., Zaitchik, B. F., Rodell, M., et al. (2018). Groundwater Withdrawals Under Drought: Reconciling GRACE and Land Surface Models in the United States High Plains Aquifer. *Water Resources Research*.
- [68] Nie, Y., Shen, Y., & Chen, Q. (2019). Combination Analysis of Future Polar-Type Gravity Mission and GRACE Follow-On. *Remote Sensing*, 11(200), 2019.
- [69] Pan Yi, YUE Jianping, Zhang Peng. An Algorithm Fusing Robust and Collinear Rank-defect Adjustment[J]. *Hydrographic Surveying and Charting*, 2017(05):26-29.

- [70] Qiao B, Zhu L, Yang R. (2019). Temporal-spatial differences in lake water storage changes and their links to climate change throughout the Tibetan Plateau[J]. *Remote Sensing of Environment*, 222:232-243.
- [71] Qiujie C, Yunzhong S, Francis O, et al. Tongji-Grace02s and Tongji-Grace02k: high-precision static GRACE-only global Earth's gravity field models derived by refined data processing strategies[J]. *Journal of Geophysical Research: Solid Earth*, 2018. S. Ni, J. Chen, C.R. Wilson, et al. (2017). Long-term water storage changes of Lake Volta from GRACE and satellite altimetry and connections with regional climate. *Remote Sensing*, 9(8): 842.
- [72] Shen Yunzhong. Algorithm Characteristics of Dynamic Approach-based Satellite Gravimetry and Its Improvement Proposals[J]. *Acta Geodaetica Et Cartographica Sinica*, 2017, 46(10): 1308-1315. DOI:10.11947/j.AGCS.2017.20170380.
- [73] Shuang Yi, Qiuyu Wang, Le Chang, et al., (2016). Changes in Mountain Glaciers, Lake Levels, and Snow Coverage in the Tianshan Monitored by GRACE, ICESat, Altimetry, and MODIS, *Remote Sens*, 8, 798.
- [74] SUI Xiaohong, ZHANG Running, WAN Xiaoyun, LI Yang. Bathymetry Prediction and Analysis Based on Satellite Altimetry Data[J]. *Spacecraft Engineering*, 2017(3):130-136.
- [75] Sun, Y., Ditmar, P., & Riva, R. (2017). Statistically optimal estimation of degree-1 and C20 coefficients based on GRACE data and an ocean bottom pressure model. *Geophysical Journal International*, 210(3), 1305-1322.
- [76] Sun, Y., Riva, R., Ditmar, P., & Rietbroek, R. (2019). Using GRACE to explain variations in the Earth's oblateness. *Geophysical Research Letters*.
- [77] Sun, Z., Zhu, X., Pan, Y., et al. (2018). Drought evaluation using the GRACE terrestrial water storage deficit over the Yangtze River Basin, China. *Science of The Total Environment*, 634, 727-738.
- [78] Tang Xinming, Chen Jiyi, Li Guoyuan, et al. Error Analysis and Preliminary Pointing Angle Calibration of Laser Altimeter on Ziyuan-3 02 Satellite. *Geomatics and Information Science of Wuhan University*, 2018, 43(11):1611-1619.
- [79] Tang, J., Cheng, H., & Liu, L. (2012). Using nonlinear programming to correct leakage and estimate mass change from GRACE observation and its application to Antarctica. *Journal of Geophysical Research: Solid Earth*, 117(B11).
- [80] Tang, Y., Hooshyar, M., Zhu, T., et al. (2017). Reconstructing annual groundwater storage changes in a large-scale irrigation region using GRACE data and Budyko model. *Journal of Hydrology*, 551, 397-406.
- [81] Tao J, JIN. (2009). Filter Technique of Removing Correlated Errors Existing in GRACE Time Variable Gravity Data. *Geomatics and Information Science of Wuhan University*, 34(12):1407-

1406.

- [82] Tao Jiang and Yan Ming Wang (2016). On the spectral combination of satellite gravity model, terrestrial and airborne gravity data for local gravimetric geoid computation. *Journal of Geodesy*, 2016, Volume 90, Issue 12, pp 1405–1418, DOI 10.1007/s00190-016-0932-7
- [83] Tian ShanChuan, Hao WefFeng, Li Fei, et al. Waveform Analysis and Retracking of Lake Level Monitoring by Satellite Altimeter Considering the Difference Between Land and Lake Reflection[J]. *Acta Geodaetica et Cartographica Sinica*, 2018, 47(4):498-507.
- [84] Wang Hong, Sun Fubao, Yang Tao, et al. Application of Jason_2 Satellite Altimetry Data to Water Level Monitoring in the Middle Reaches of the Yangtze River[J], *Ecology and Environmental Monitoring of Three Gorges*, 2018, v.3; No.10(03):52-58.
- [85] Wang, L., Chen, C., Du, J., et al.(2017). Detecting seasonal and long-term vertical displacement in the North China Plain using GRACE and GPS. *Hydrology and Earth System Sciences*, 21(6), 2905-2922.
- [86] Wang, S.Y., Chen, J. L., Wilson, C. R., et al. (2017). Reconciling GRACE and GPS estimates of long-term load deformation in southern Greenland. *Geophysical Journal International*, 212(2), 1302-1313.
- [87] Wen H, Huang Z, Wang Y, et al. (2016).Independent Component Analysis of Water Storage Changes Interpretation over Tibetan Plateau and Its Surrounding Areas. *Acta Geodaetica Et Cartographica Sinica*, 45(1):9-15.
- [88] Wen Jingchuan, Zhao Hongli, Jiang YunZhong,et al. Research on the quality screening method for satellite altimetry data-take Jason-3 data and Hongze Lake as an example[J].*South-to-North Water Transfers and Water Science & Technology*, 2018, 16(3):194-200.
- [89] Wenli Wang, Chunxi G, Li D, et al. Elevation change analysis of the national first order leveling points in recent 20 years[J]. *Acta Geodaetica et Cartographica Sinica*, 2019,48(1):1-8.DOI:10.11947/j.AGCS.2019.20170589.
- [90] Wu, Q., Si, B., He, H., et al. (2019). Determining Regional-Scale Groundwater Recharge with GRACE and GLDAS. *Remote Sensing*, 11(2), 154.
- [91] Xing, W., Wang, W., Shao, Q., et al. (2018). Estimating monthly evapotranspiration by assimilating remotely sensed water storage data into the extended Budyko framework across different climatic regions. *Journal of Hydrology*.
- [92] Yang Lei, Zhou Xinghua, Xu Quanjun, et al. Research status of satellite altimeter calibration[J]. *Journal of Remote Sensing*, 2019,23(3): 392–407.
- [93] YU Jin-Hai, ZENG Yan-Yan, ZHU Yong-Chao et al .2015.A recursion arithmetic formula for Legendre functions of ultra-high degree and order on every other degree.*Chinese Journal Of Geophysics*,58(3): 748-755,doi: 10.6038/cjg20150305

- [94] Zeng, R., & Cai, X. (2018). Hydrologic observation, model, and theory congruence on evapotranspiration variance: Diagnosis of multiple observations and land surface models. *Water Resources Research*.
- [95] Zhai Zhenhe, Sun Zhongmiao, Xiao Yun, LI Fang. Two-Satellites Tandem Mode Design and Accuracy Analysis of Gravity Field Inversion for Independent Marine Altimetry Satellite[J]. *Geomatics and Information Science of Wuhan University*, 2018,43(07),1030-1035+1128.
- [96] Zhai Zhenhe, Sun Zhongmiao, Xiao Yun, LI Fang. Two-Satellites Tandem Mode Design and Accuracy Analysis of Gravity Field Inversion for Independent Marine Altimetry Satellite[J]. *Geomatics and Information Science of Wuhan University*, 2018,43(07),1030-1035+1128.
- [97] Zhang Guo, Li Shaoning, Huang Wenchao, et al. Geometric Calibration and Validation of ZY3-02 Satellite Laser Altimeter System[J]. *Geomatics & Information Science of Wuhan University*, 2017(11):92-99.
- [98] Zhang Wenhao, Li Song, Zhang Zhiyu, et al. Using waveform matching to precisely locate footprints of a satellite laser altimeter[J]. *Infrared and Laser Engineering*, 2019, 46(01):310-317.
- [99] Zhang Y, Chen C. Forward calculation of gravity and its gradient using polyhedral representation of density interfaces: an application of spherical or ellipsoidal topographic gravity effect[J]. *Journal of Geodesy*, 2018, 92(2):205-218.
- [100] Zhang, H., & Sun, Y. (2018). Climate-driven seasonal geocenter motion during the GRACE period. *Acta Geophysica*, 66(2), 223-232.
- [101] Zhang, T., Shen, W., Pan, Y., et al. (2018). Study of seasonal and long-term vertical deformation in Nepal based on GPS and GRACE observations. *Advances in Space Research*, 61(4), 1005-1016.
- [102] Zhang, Z.Z., Chao, B. F., Lu, Y., et al. (2009). An effective filtering for GRACE time-variable gravity: Fan filter. *Geophysical Research Letters*, 36(17).
- [103] Zhang, Z.-Z., Chao, B. F., Lu, Y., et al. (2009). An effective filtering for GRACE time-variable gravity: Fan filter. *Geophysical Research Letters*, 36(17).
- [104] Zhibin X , Shanshan L I , University I E . The 3D Gravity Vectors Method in China Land and Ocean Quasigeoid Determination[J]. *Acta Geodaetica et Cartographica Sinica*, 2018,47(5):575-583.DOI:10.11947/j.AGCS.2018.20170076.
- [105] Zhong, M., Duan, J., Xu, H., et al. (2008). Trend of China land water storage redistribution at medi- and large-spatial scales in recent five years by satellite gravity observations. *Science Bulletin*, 54(5), 816-821.
- [106] Zhong, Y., Zhong, M., Feng, W., et al. (2018). Groundwater Depletion in the West Liaohe River Basin, China and Its Implications Revealed by GRACE and In Situ Measurements. *Remote*

Sensing, 10(4), 493.

- [107]Zhou Chunxia, Zhao Qiuyang, Qiang Qiang. Detection of Antarctic Subglacial Lakes Activities Using ICESat Altimetry Data[J]. Geomatics and Information Science of Wuhan University, 2018, 43(10):1458-1464+1471.
- [108]Zhou, H., Luo, Z., Tangdamrongsub, N., et al. (2018). Identifying Flood Events over the Poyang Lake Basin Using Multiple Satellite Remote Sensing Observations, Hydrological Models and In Situ Data. Remote Sensing, 10(5), 713.
- [109]ZOU Xian-Cai, LI Jian-Cheng .2016.Study on the earth gravity modeling by GOCE in individual accelerometer mode.Chinese Journal Of Geophysics,59(4): 1260-1266,doi: 10.6038/cjg20160408
- [110]ZOU Xian-Cai, ZHONG Lu-Ping, LI Jian-Cheng .2016.Simultaneous solution for precise satellite orbit and earth gravity model.Chinese Journal Of Geophysics,59(7): 2413-2423,doi: 10.6038/cjg20160708

3. Positioning and Application

3.1 Comprehensive PNT architecture

In China, a comprehensive PNT architecture based on the Beidou system was widely discussed during the past two or three years. The core idea of comprehensive positioning, navigation and time (PNT) is the technique that uses all the available resources to provide PNT services in the whole area, including inside and outside door, air space, underwater and underground, which does not solely rely on the GNSS. In fact, as early as 2008, the U.S. had completed the National PNT Architecture Study (Final report) to develop a comprehensive National PNT Architecture as a framework for developing future PNT capabilities and supporting infrastructure.

Prof. Yang Yuanxi as one of representative PNT scholars in China has made great efforts on establishing the national comprehensive PNT architecture of China. In his several representative publications, the definition and basic concepts of the comprehensive PNT were widely presented, all possible signal sources and the core technologies related to the comprehensive PNT were both analyzed, including the integration of the multiple sensors and adaptive data fusion for multiple PNT signals. It is emphasized that the information of the comprehensive PNT should be from “multiple sources based on different physical principles”, the control system should be operated by voluntary users based on cloud platform, the user terminals or sensors should be “deeply integrated” and the PNT information should be “adaptively fused” and serve mode might be based on cloud platform. The comprehensive PNT system should meet the robust availability, continuity, high accuracy and reliability with unified geodetic datum and time datum. The main academic contributions may be summarized as follows:

1) Comprehensive PNT

The concept and structure of the comprehensive PNT was discussed. It shows that the comprehensive PNT should be based on different principles of multiple PNT information sources. The data processing may be located at the control terminal of the cloud platform in the near future. The multi PNT data should be deeply integrated within the unified geodetic datum and time datum to provide the robust, available, continuous and reliable PNT information.

2) Micro-PNT

The investigation shows that micro-PNT should include multi-GNSS integration and micro components of navigation and timing, and the PNT outputs should have the unified coordinate datum and time scale. Relative to the comprehensive PNT, Micro-PNT mainly focuses on the personalized micro terminals. Besides the miniaturizing each of the PNT components, micro-PNT should be integration of the micro sensors, adaptive data fusion and self-calibration of each

component.

3) Resilient PNT

The definition and architecture of resilient PNT are proposed and discussed. It shows that the resilient PNT should be divided into the resilient sensors integration, resilient functional model and resilient stochastic model to reduce the various model errors influences.

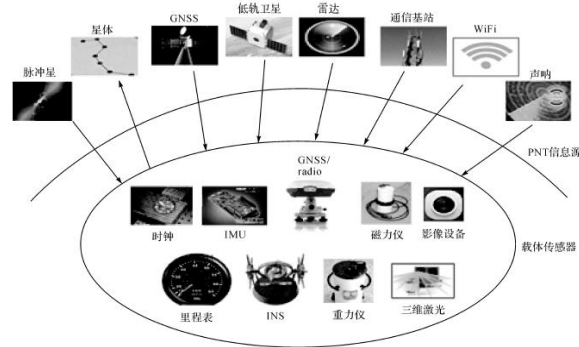


Fig. 3.1 Resilient PNT architecture

4) Underwater PNT

Prof. Xu Jiang analyzed the underwater PNT system and key technologies. The underwater users of PNT system are classified. The gap between requirements of underwater users and the current underwater PNT system is analyzed.

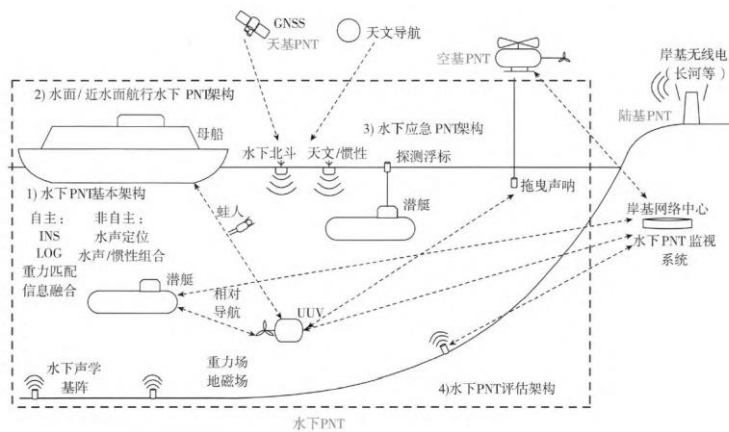


Fig. 3.2 Underwater PNT architecture

The construction conditions of underwater PNT system and the construction plans of some countries are studied. On this basis, the development direction of underwater PNT system is analyzed. In view of the characteristics of underwater PNT system, key technologies such as inertial technology, gravity/geomagnetic matching technology, acoustic navigation technology and evaluation technology are investigated.

3.2 BDS Triple-frequency PPP

The triple-frequency BDS signals were fully exploited in term of modeling and assessing of precise point positioning with BDS data. Triple-frequency PPP models include “Ionospheric Free PPP (IF-PPP)” and “Uncombined PPP (UC-PPP)”. The observation model and stochastic model were extended to accommodate the third frequency. Comparative analyses show that both dual- and triple-frequency static BDS PPP can reach an accuracy of a few millimeters in horizontal. However, the vertical positioning accuracy of BDS PPP is significantly worse than GPS and shows systematic biases of 2–3 cm.

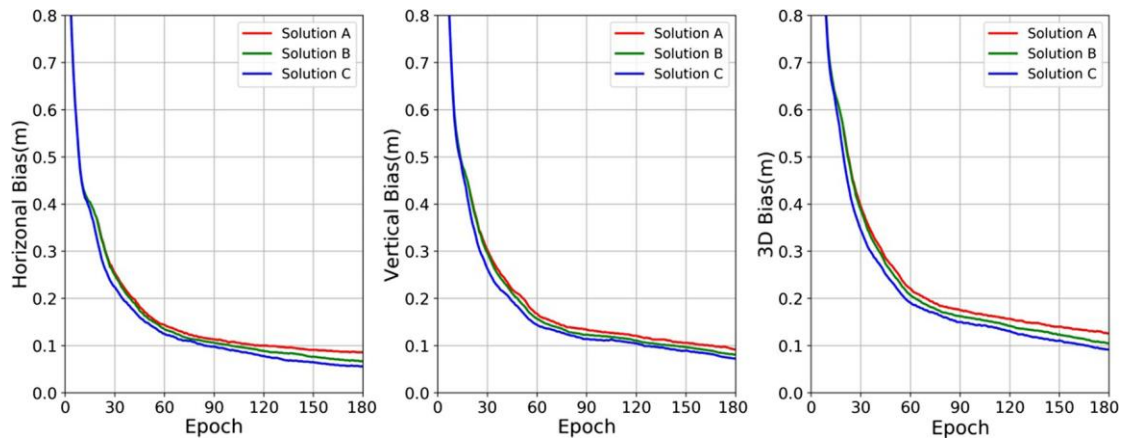


Fig. 3.3 Average convergence series of BDS PPP from Li (2018)

In kinematic PPP tests, an accuracy of 3–4 cm in horizontal and 8–10 cm vertically is achievable with the current BDS constellation. Such an accuracy is worse than GPS by a factor of two due to its poorer geometry and worse orbit and clock quality. Compared to dual-frequency PPP, the benefits of third frequency would be significant in situations where there is poor tracking and contaminated observations on frequencies B1 and B2. This implies a stronger robustness for the triple-frequency PPP.

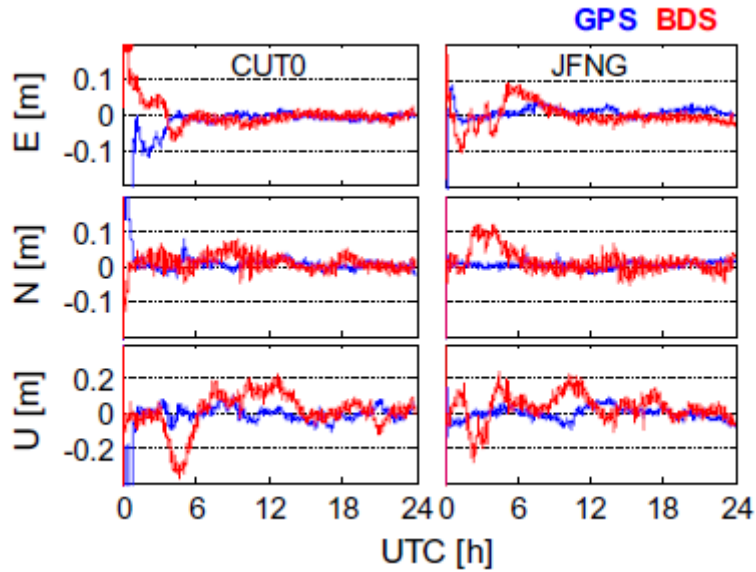


Fig. 3.4 Comparisons of the BDS/GPS kinematic positioning performance from Guo (2016)

3.3 Triple-frequency observations analysis

With the third frequency, receiver phase biases (RPBs) arise that need to be taken into account in triple-frequency PPP. Dynamics features of RPBs were investigated by detailed analyzing estimates of L1 and wide-lane (WL) RPBs for a number of short and zero baselines repeatedly measured in a variety of multipath environments. RPBs were estimated by means of a real-time estimator like Kalman filter in the context of PPP-RTK. The estimates show noticeable fluctuations, attributable to random measurement noise and a combination of multipath and ambient temperature. The high-frequency noise, responsible for a large portion of fluctuations in the epoch-by-epoch estimates, is induced mainly by the random measurement noise. One can simply suppress it by filtering. The low-frequency signal, observed in the low-pass-filtered, epoch-by-epoch estimates, is largely due to multipath. One can opt for the use of sidereal filtering as a mitigation measure. Moreover, a fraction of this signal is caused by changes in ambient temperature. It follows from the zero baseline experiment that the sensitivity of the epoch-by-epoch estimates of WL RPBs to the ambient temperature ranges from 0.007 to 0.009 cycles per degree Celsius. With these factors removed, the L1 residuals can be modeled as a random walk process, while the WL residuals become time constant.

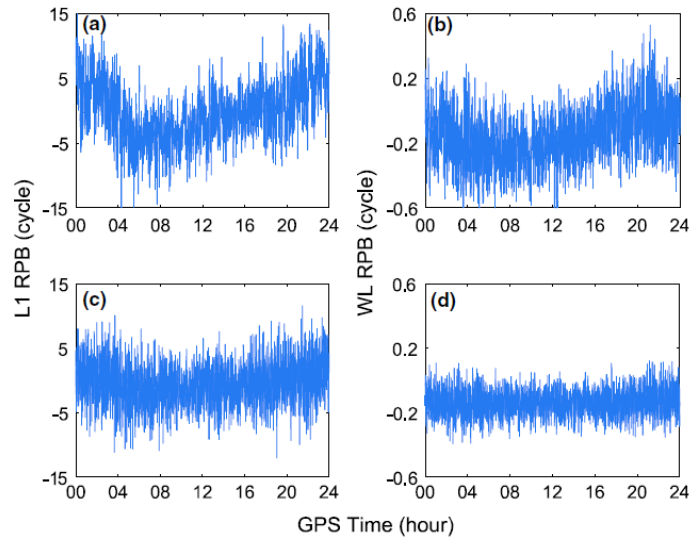


Fig. 3.5 Time series (24 h) of epoch-by-epoch estimates of L1 and WL RPBs for baselines from zhang (2018)

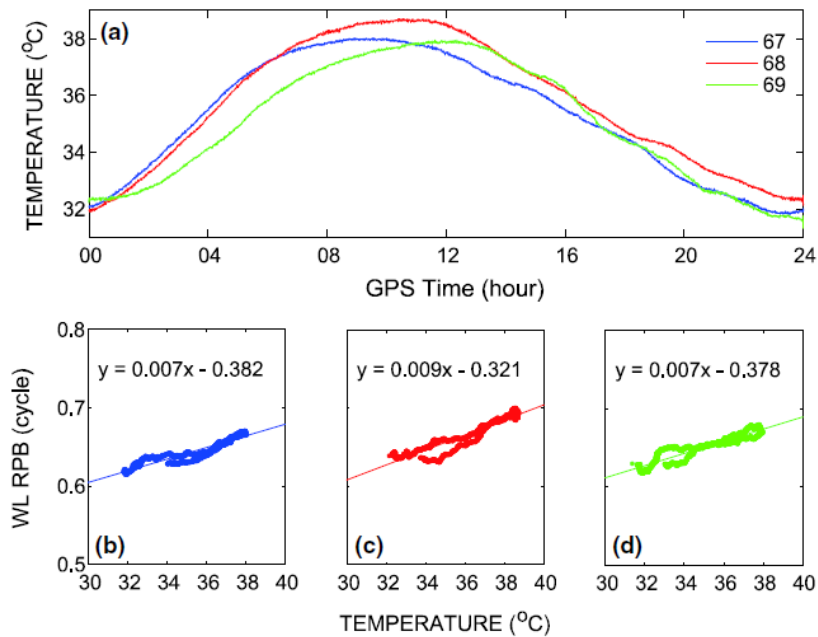


Fig. 3.6 Time series of ambient temperatures of WL RPBs from zhang (2018)

3.4 Indoor Positioning

Currently, Indoor positioning is one of the hot research topics in academic and industrial society approach. However, affected by the complexity of the indoor spaces, it is still challenging to achieve accurate, effective, full coverage and real-time positioning solution indoors. With the popularity of smart phones and the rapid development of MEMS sensors in recent years, the radio frequency(RF) technologies and the sensors technologies were used for indoor positioning built-in smartphone.

As one of RFs, WIFI indoor positing accuracy could reach 2-5m by using received signal

strength index (RSSI) and channel state information (CSI); Bluetooth indoor positioning accuracy could reach 2-4m by using RSSI. Among sensors technologies, pedestrian dead reckon (PDR) was a reliable way for indoor positioning. PDR employed an accelerometer to detect the number of steps and measure the walking speed, a magnetometer and gyroscope to determine the heading azimuth. Then, a relative displacement of pedestrians was estimated by pace and heading.

As same as navigation satellites system, pseudo-satellite network was deployed to indoor positioning with a horizontal accuracy of 0.3-1m in assist of ranging observations. There will be more than 4 indoor pseudo-satellites send L1/L2 carrier phase and CA pseudo-range signals. GNSS chip in smartphone received pseudo-satellites signals and outputted positioning results.

With the rapid development of 5G networks, the denser 5G networks equipped smart antennas with array antennas. In the context of the future 5G densification network, the range and DOA (Direction of Arrival) was obtained by the array antenna of the node. 0.5-1m location accuracy can be achieved by smartphone in 5G networks.

Bibliography

- [1] B Wang et al. A Characteristic Parameter Matching Algorithm for Gravity-aided Navigation of Underwater Vehicles. IEEE Transactions on Industrial Electronics. 2018. 10.1109/TIE.2018.2831171
- [2] Chen Ruizhi, Chen Liang (2017) Indoor positioning with smart phones: the State-of-the-art and the challenges. Acta Geodaetica et Cartographica Sinica 46(10):1316-1326
- [3] Deng Zhongliang, Yin Lu, Tang Shihao et al (2018) A Survey of key technology for indoor positioning. Navigation positioning and timing 5(03):14-23
- [4] Geng J, Shi C (2016) Rapid initialization of real-time PPP by resolving undifferenced GPS and GLONASS ambiguities simultaneously. Journal of Geodesy 91(4):1-14
- [5] Guo F, Zhang X, Wang J et al (2016) Modeling and assessment of triple-frequency BDS precise point positioning. J Geod 90(11):1223–1235
- [6] Han Y, Wang B et al. A Combined Matching Algorithm for Underwater Gravity Aided Navigation. IEEE/ASME Transactions on Mechatronics. 10.1109/TMECH.2017.2774296
- [7] Han Y, Wang B et al. A Matching Algorithm based on Nonlinear Filter and Similarity Transformation for Gravity Aided Underwater Navigation. IEEE/ASME Transactions on Mechatronics. 2018, 23(2): 646-654.
- [8] Li P, Zhang X, Ge M, Schuh H (2018) Three-frequency BDS precise point positioning ambiguity resolution based on raw observables. J Geod 92(12):1357–1369
- [9] Li B (2016). Stochastic modeling of triple-frequency BeiDou signals: estimation,

- assessment and impact analysis. *Journal of Geodesy* 90: 593-610
- [10] Wei Baoguo, He Zhonglong(2017) *Journal of Huazhong University of Science and Technology* 45(01):113-117
- [11] Wu L et al, Performance Evaluation and Analysis for Gravity Matching Aided Navigation. *Sensors*, 2017, 17(4), 769
- [12] YANG Yuanxi. Concepts of Comprehensive PNT and Related Key Technologies[J]. *Acta Geodactica et Cartographica Sinica*, 2016, 45(5):505-510. DOI:10.11947/j.AGCS.2016.20160127
- [13] YANG Yuanxi, Li Xiaoyan. Micro-PNT and Comprehensive PNT[J]. *Acta Geodaetica et Cartographica Sinica*, 2017, 46(10):1249-1254. DOI:10.11947/j.AGCS.2017.20170249
- [14] YANG Yuanxi, XU Tianhe, XUE Shuqiang. Progresses and Prospects in Developing Marine Geodetic Datum and Marine Navigation of China[J]. *Acta Geodaetica et Cartographica et Cartographica Sinica*, 2017, 46(1):1-8. DOI:10.11947/j.AGCS.2017.20160519.
- [15] YANG Yuanxi. Resilient PNT Concept Frame[J]. *Acta Geodaetica et Cartographica Sinica*, 2018, 47(7):893-898. DOI:10.11947/j.AGCS.2018.20180149
- Y Han, B Wang, Z Deng et al., A Mismatch Diagnostic Method for TERCOM-based Underwater Gravity Aided Navigation. *IEEE Sensors Journal*. 2017, 17(9): 2880-2888.
- [16] Zhang B, Liu T, Yuan Y (2018) GPS receiver phase biases estimable in PPP-RTK networks: dynamic characterization and impact analysis. *J Geod* 92(6):659–674

4. Researches and Application of Chinese Geodetic Observing System

In cooperation with the International Association of Geodesy (IAG), China has carried out the millimeter-scale high-precision surface monitoring of changes in the Earth's space environment by constructing the Chinese Geodetic Observing System (CGOS); participating in Global Geodynamic Project (GGP) observation and research project organized by the International Union of Geodesy and Geophysics (IUGG). In recent years, with the support of the National Natural Science Foundation of China and major national R&D projects, China has used modern geodetic techniques to conduct research on global environmental and climate change monitoring and inversion, tectonic and seismic mechanisms, and geological hazard warnings, and have got some important results.

4.1 Data processing method

For ill-conditioned problems, Zhu et al. (2016) selected a smaller singular value eigenvector to construct a regularization matrix, and proposed a new reliable parameter estimation method. Lin and Zhu (2017) corrected the variance of the singular value by comparison. The relationship between quantity and deviation is introduced, and the improved ridge estimation method with singular value correction limit is given, which effectively improves the solution efficiency and reliability of ridge estimation. Liu et al. (2017) proposed a new bias. The iterative estimation method transforms the iterative formula into an analytical expression that is easy to solve, and proves the convergence of the iterative formula in the correction factor. Xu et al. (2017) proposed an adaptive method based on the classical Laplacian smoothing constraint idea and smooth constraint algorithm. In the aspect of uncertainty data processing, Wang et al. (2017) proposed the adjustment criterion of the smallest square error of random error and uncertainty error under bounded uncertainty error constraint, and gave an iterative algorithm for uncertainty adjustment model. Wei et al. (2016) based on measurement uncertainty theory and fuzzy mathematics, constructed a functional model for uncertainty assessment of measurement data with unknown measurement uncertainty, and proposed "fuzzy entropy measure" as a function model. The optimal criterion and the corresponding algorithm are established. Wei et al. (2018) described the uncertainty of deformation prediction in the form of probability distribution, and proposed a kind of a priori information and uncertain information of parameters into the objective function according to Bayesian law.

In terms of overall adjustment, Fang et al. (2016) proposed a hybrid global least squares estimation method based on nonlinear Gaussian-Helmert model. Tao et al. (2016) proposed observation vectors and coefficient matrices for models. The idea of classifying and weighting the observed elements avoids the influence of the error estimation bias and the random model error on the equivalence weight function; the observation vector and the coefficient matrix elements are studied (Wang et al. 2016, 2017). In order to improve calculation efficiency of parameter estimation,

an algorithm for multivariate weighted total least squares adjustment based on Newton method is derived. The relationship between the solution of this algorithm and that of multivariate weighted total least squares adjustment based on Lagrange multipliers method is analyzed. According to propagation of cofactor, 16 computational formulae of cofactor matrices of multivariate total least squares adjustment are also listed. By adding the relative weight ratio to the adjustment criterion, the contribution of the observation vector and the random element of the coefficient matrix to the model parameter estimation is adaptively adjusted, and the pre-test unit weight variance for determining the relative weight ratio is given. The method and the discriminant function minimize the iterative algorithm. Yao et al. (2017) proposed a new global least squares algorithm for AR models. By introducing observations that are not present in the observation vector and containing errors as virtual observations, the corrections corresponding to the design matrix and the unknown parameters are initially set. The value product is rewritten, which effectively overcomes the problem that the same parameter in the AR model has different correction points at different positions, and can perform accuracy evaluation.

4.2 Monitoring of water storage variants and deformation

Wang et al. (2017) used the CORS station network to monitor the changes in groundwater reserves in the Three Gorges area. The results were then compared with the water level from groundwater monitoring wells. The comparison indicates that it is possible to calculate the temporal and spatial variation of groundwater with high precision based on the continuous observation data of CORS and a small amount of gravity stations.

Sun et al. proposed a new method for detecting glacier terrain and glacier surface change based on X-band terrain SAR satellite digital elevation measurement sister star (TanDEM-X) dual-station InSAR, which significantly improved the efficiency of phase unwrapping and glacier topography. Taking the western mountain glaciers in the Qilian Mountains of the Qinghai-Tibet Plateau as an example, the glacial topography with a spatial resolution of 0.7m and an elevation accuracy of 0.7m was obtained for the first time. This technology validates the application potential of Landsat-7 SLC-OFF image in mountain glaciers flow monitoring, which provides a new data source for glacier monitoring after 2003, and is of great significance for long-term and continuous monitoring of mountain glacier movement.

Yang presents a method for deriving time series three-dimensional (3-D) displacements of mining areas from a single-geometry Interferometric Synthetic Aperture Radar (InSAR) dataset (hereafter referred to as the SGI-based method). And The SGI-based method not only extends the SIP-based method to time series 3-D displacement retrieval from a single-geometry InSAR dataset, but also limits the uncertainty propagation from InSAR-derived deformation to the estimated 3-D

displacements.

4.3 Geodetic inversion

The geodetic inversion method has been further developed. Xu et al. (2016) proposed a seismic coseismic slip distribution inversion method based on variance component estimation, which can simultaneously determine the relative weight ratio and smoothing factor of different types of data. Yin et al. (2016) proposed a hybrid inversion method based on surface tomography. Wang et al. (2016) proposed an adaptive regularization method for coseismic sliding distribution inversion, which can simultaneously process regularization matrices and observation error; Wang et al. (2017) proposed the total minimum two of coseismic sliding distribution inversion. Multiplication method can simultaneously process the Green's function matrix and observation error. Fan (2017) studied the multi-source data and ill-conditioned inversion problem method, and proposed an adaptive smoothing constraint method for coseismic sliding distribution inversion; Yi (2017) proposed the generalized Bayesian information criterion to carry out the optimization of multi-source data joint inversion model for seismic source rupture process. Li (2017) studied the high-frequency GNSS denoising method and successfully applied it to the focal mechanism solution. Xu et al. (2018) proposed a spectrum expansion method for sliding distribution inversion, using geodetic data to study large scale Red zone ruptures depth of the earthquake. The joint inversion of multiple data is still the trend of geodetic inversion. Huang et al. (2017) used GPS, InSAR, and optical and SAR image migration data to study the El Mayor-Cucapah seismic fault geometry and slip distribution in 2010. Xu (2017) used InSAR and SAR image migration data to invert the 2016 Chiloé earthquake Source parameters and sliding distribution. Yue et al. (2017) used GPS, strong seismometer, InSAR and SAR and optical image migration data to invert the rupture process of the 2015 Kumamoto earthquake sequence. Wang (2018) combined with GPS, InSAR, SAR image bias Migration, geological, seismic and tsunami wave data inversion of the 2016 Kaikoura earthquake slip distribution and rupture process.

Using satellite gravity data, Feng et al. studied the groundwater reserves in North China (including Beijing, Tianjin, Hebei, and Shanxi) at a rate of 2.5 cm/yr from 2003 to 2010, which is consistent with the monitoring results of 40 wells in North China. The results of quantitative calculations indicate that the region is depleted by approximately 71 ± 1 billion tons of groundwater per year, a result that is more than three times earlier based on shallow groundwater statistics. The study also successfully found the inter-annual variability signal characteristics of groundwater reserves in North China. Using the GRACE satellite gravity data, the seasonal seawater quality change signals in the Red Sea region were successfully obtained, and the seawater quality change was the main cause of the mean sea level change in the region.

Peng et al. (2016) used GRACE satellite data to quantitatively estimate the quality change of the Antarctic ice sheet from 2002 to 2011. By applying the new Forward-Modeling method, the spatial accuracy of the GRACE satellite data in this region is improved, and a more accurate variation of the Antarctic ice sheet is obtained. Mu et al. proposed a new method of regularization. Using GRACE data, the spatial distribution of ice and snow ablation rate of Antarctic and Greenland is more accurate, and the regional variation of ice and snow ablation is refined.

4.4 Seismological applications of geodesy

In the observational study of seismic crustal deformation field and gravity field, with the development of modern geodetic techniques such as GNSS and gravity satellites, the coseismic impact of large earthquakes on the global scale can be directly monitored, thus greatly promoting the global scale. In recent years, the quantitative calculation of the influence of spherical dislocation theory on coseismic evolution has gradually extended from the early surface of the Earth to the interior of the Earth, and more realistically considers the influence of the curvature of the Earth and the layered factors (Dong et al., 2014, 2016). Recently, by introducing the asymptotic solution of the radial function, the solution of the coseismic displacement, stress, strain and gravity at any point in the Earth model caused by the point source dislocation is realized. At the same time, it is also directly obtained. Analytical method is used to solve the calculation method of vertical coseismic displacement in the uniform medium earth model caused by the strike-slip source (Dong and Sun, 2017). In the observational study of earthquake rupture and post-earthquake residual slip, the geodetic observations such as GNSS and InSAR are used to more accurately invert the spatial distribution of the earthquake rupture coseismic dislocation and post-earthquake residual slip, and the occlusion segment of the fault (Zhao et al., 2017; Wang and Fialko, 2018; Jiang et al., 2018). In the inversion determination of the viscoelastic medium parameters of the Earth's lithosphere, using the more refined GPS and InSAR post-earthquake relaxation deformation evolution results, a more reliable transient and steady-state viscosity coefficient of the upper mantle were obtained by the inversion. Opportunities in the lithospheric structure and dynamics of the earthquake zone are provided (Zhao et al., 2017; Wang and Fialko, 2018; Jiang et al., 2018). In the seismology of high-frequency GNSS, the accuracy of obtaining seismic waveforms using multimode high-frequency GNSS (BDS+GPS) observation data has been significantly improved, especially the seismic velocity obtained by using variometric processing method and BDS+GPS dual-mode data. The GPS results with a single waveform increase by about 20% in accuracy (Geng et al., 2016).

Lu et al. conducted InSAR monitoring and simulation studies on the volcanic activity of the Aleutian volcanic group for nearly 20 years, which is of great significance for understanding the mechanical mechanism of fire magma and the prediction of eruption disasters. The data were used

to monitor the surface two-dimensional deformation field in the Taiyuan Basin, and the relationship between the monitoring results and the surrounding fractures and groundwater extraction was analyzed. Zhang et al. proposed an improved time series InSAR technique—multi-master image coherent target small baseline interference technique (MCTSB-InSAR), which monitors the land subsidence information of the Beijing-Tianjin-Hebei region during three periods from 1992 to 2014.

GNSS has continuous real-time dynamic monitoring capability with high time resolution for real-time dynamic deformation results. Based on the analysis of the relationship between the accuracy of the landslide monitoring, the retest cycle and the speed, Wang Li discussed the key issues of the accuracy, scope and constraints of the three GPS rapid positioning techniques in the dynamic deformation monitoring of landslide hazards. Zhou et al. used GNSS technology to effectively monitor the landslides of islands, explore the induced factors of landslides, and achieve the purpose of disaster prevention and mitigation in island areas. Zhang et al. (2019) proposed a known load removal recovery method for the time-varying gravitational field and load deformation field refinement of the CORS station network, and carried out the geological disaster precursor capture research using the CORS station network. Su et al. (2019) proposed an iterative PCA method which takes both the spatial correlation of postseismic deformation and overall modeling into account, and proved its advantages in estimating more robust parameters with the simulated data.

Bibliography

- [1] Dang Yamin, Yang Qiang, Wang Wei. Geodetic Method and Application on Monitoring the Stability of Regional Geological Environment [J]. *Acta Geodaetica et Cartographica Sinica*, 2017, 46(10):1336-1345
- [2] Dong J, Sun W, Zhou X, Wang R. An analytical approach to estimate curvature effect of coseismic deformations. *Geophys J Int* ,2016,206:1327–1339
- [3] Fan Q, Xu C, Yi L, et al. Implication of adaptive smoothness constraint and Helmert variance component estimation in seismic slip inversion[J]. *Journal of Geodesy*, 2017(1):1-15.
- [4] Fan Qingbiao. Multi-source data multi-constrained ill-conditioned inversion problem method and application [D]. Wuhan: Wuhan University, PhD thesis, 2017.
- [5] FANU Xing, ZENU Wenxian, LIU Jingnan, Mixed LS-TLS Estimation Based on Nonlinear Gauss-Helmert Mode[J]. *Acta Geodaetica et Cartographica Sinica*, 2016, 45(3):291-296.
- [6] Geng, T., et al. (2016). "Real-time capture of seismic waves using high-rate multi-GNSS observations: Application to the 2015Mw 7.8 Nepal earthquake." *Geophysical Research Letters* 43(1): 161-167.
- [7] Huang Guanwen, Huang Guanwu, Du Yuan, et al. A low cost real-time monitoring system

- for landslide deformation with Beidou cloud [J]. *Journal of Engineering Geology*, 2018, 26(4): 1008–1016.
- [8] Huang M H, Fielding E J, Dickinson H, et al. Fault geometry inversion and slip distribution of the 2010 Mw 7.2 El Mayor - Cucapah earthquake from geodetic data[J]. *Journal of Geophysical Research: Solid Earth*, 2017, 122(1): 607-621.
- [9] Jiang Zhaoying, Liu Guolin, Yu Shengwen. A New Iterative Estimator Method Based on Liu Estimator for Ill-Posed Equations [J]. *Geomatics and Information Science of Wuhan University*, 2017, 42(8):1172-1178.
- [10] Jiang, Z., Yuan, L., Huang, D., Yang, Z., & Hassan, A. (2018). Postseismic deformation associated with the 2015 mw 7.8 gorkha earthquakes, Nepal: investigating ongoing afterslip and constraining crustal rheology. *Journal of Asian Earth Sciences*. DOI: 10.1016/j.jseaes.2017.12.039
- [11] Li Yanyan. High-frequency GNSS denoising method and its application in focal mechanism solution inversion [D]. Wuhan: Wuhan University, PhD thesis, 2017.
- [12] Lin Dongfang, Zhu Jianjun, Song Yingchun, et al. Regularized singular value decomposition parameter construction method [J]. *Acta Geodaetica et Cartographica Sinica*, 2016, 45(8):883-889.
- [13] Lin Dongfang, Zhu Jianjun. Improved Ridge Estimation Method with Singular Value Correction Limits [J]. *Geomatics and Information Science of Wuhan University*, 2017, 42(12):1834-1839.
- [14] Mu D, Yan H, Feng W, et al. GRACE leakage error correction with regularization technique : case studies in Greenland and Antarctica [J]. *Geophys Int J*, 2017, 208(3): 1775-1786.
- [15] Peng P, Zhu Y, Zhong M, et al. Ice mass variation in Antarctica from GRACE over 2002-2011 [J]. *Marine Geodesy*, 2016, DOI: 10. 1080/01490419. 2016. 11456.
- [16] Su I. N, Gan W J, Ghang Y, et al. 2019. Iterative PCA estimation and its application to postseismic deformation from GPS coordinate time series. *Chinese J. Geophys.* (in Chinese), 2019,62(3):940-949
- [17] Tao Yeqing, Gao Jingxiang, Yao Yifei. Total Residual Least Squares Estimation Based on Median Method [J]. *Acta Geodaetica et Cartographica Sinica*, 2016, 45(3):297-301.
- [18] Wang Leyang, Li Haiyan, Wen Yangmao, et al. Total Least Squares Method for Seismic Coseismic Sliding Distribution Inversion [J]. *Acta Geodaetica et Cartographica Sinica*, 2017, 46(3):307-315.
- [19] Wang Leyang, Wen Guisen. Non-negative least squares variance component estimation of Partial EIV model [J]. *Acta Geodaetica et Cartographica Sinica*, 2017, 46(7):857-865.
- [20] Wang Leyang, Zhao Ying, Chen Xiaoyong, et al. Newton's solution to multivariate total least

- squares problem [J]. *Acta Geodaetica et Cartographica Sinica*, 2016, 45(4):411-417.
- [21] Wang Qisheng, Yang Dehong, Yang Tengfei. A new method for parameter estimation of EIV model [J]. *Geomatics and Information Science of Wuhan University*, 2016, 41(3):356-360.
- [22] Wang T, Wei S, Shi X, et al. The 2016 Kaikōura earthquake: Simultaneous rupture of the subduction interface and overlying faults[J]. *Earth and Planetary Science Letters*, 2018, 482: 44-51.
- [23] Wang Wei, Zhang Chuanyin, Liang Shiming, Yang Qiang et al. Monitoring of the temporal and spatial variation of groundwater storage in the Three Gorges area based on the CORS network[J].*Journal of Applied Geophysics*, 2017, 146(2017): 160-166.
- [24] Wang Zhizhong, Chen Danhua, Song Yingchun. Adjustment algorithm with uncertainty [J]. *Acta Geodaetica et Cartographica Sinica*, 2017, 46(7):834-840.
- [25] Wang, K., & Fialko, Y. (2018). Observations and modeling of coseismic and postseismic deformation due to the 2015 Mw 7.8 Gorkha (Nepal) earthquake. *Journal of Geophysical Research: Solid Earth*, 123. <https://doi.org/10.1002/2017JB014620>
- [26] Wei Guanjun, Dang Yamin, Zhang Chuanyin, et al. Deformation Probability Forecasting Method Considering the Influence of Uncertainty [J]. *Acta Geodaetica et Cartographica Sinica*, 2017, 46(4):526-532.
- [27] Wei Guanjun, Dang Yamin, Zhang Chuanyin. Minimum Fuzzy Entropy Algorithm for Measurement Data Uncertainty Measurement [J]. *Geomatics and Information Science of Wuhan University*, 2016, 41(12):1677-1682.
- [28] Xu Caijun, Deng Changyong, Zhou Lijun. Seismic coseismic slip distribution inversion using variance component estimation [J]. *Geomatics and Information Science of Wuhan University*, 2016, 41(1):37-44.
- [29] Xu P. The effect of errors-in-variables on variance component estimation[J]. *Journal of Geodesy*, 2016, 90(8):1-21.
- [30] Xu W. Finite - fault Slip Model of the 2016 Mw 7.5 Chiloé Earthquake, Southern Chile, Estimated from Sentinel - 1 Data[J]. *Geophysical Research Letters*, 2017, 44(10): 4774-4780.
- [31] Xu X, Sandwell D T, Bassett D. A spectral expansion approach for geodetic slip inversion: implications for the downdip rupture limits of oceanic and continental megathrust earthquakes[J]. *Geophysical Journal International*, 2018, 212(1): 400-411.
- [32] Yao Yibin, Xiong Zhaohui, Zhang Bao, et al. New solution to AR model considering design matrix error [J]. *Acta Geodaetica et Cartographica Sinica*, 2017(11):1795-1801.
- [33] Yi Lei. Optimization of multi-source data joint inversion mode for earthquake source rupture process [D]. Wuhan: Wuhan University, PhD thesis, 2017.
- [34] Yin Z, Xu C, Wen Y, et al. A new hybrid inversion method for parametric curved faults and its

- application to the 2008 Wenchuan (China) earthquake[J]. *Geophysical Journal International*, 2016, 205(2): 954–970.
- [35] Yue H, Ross Z E, Liang C, et al. The 2016 Kumamoto Mw= 7.0 Earthquake: A Significant Event in a Fault–Volcano System[J]. *Journal of Geophysical Research: Solid Earth*, 2017, 122(11): 9166-9183.
- [36] Yun Shi, Peiliang Xu, Junhuan Peng. A computational complexity analysis of Tienstra’s solution to equality-constrained adjustment. *Stud. Geophys. Geod.*, 61 (2017), 601–615, DOI: 10.1007/s11200-016-0296-8.
- [37] Zhang Chuanyin, Li Aiqin, Dang Yamin, et al. A method of tracking and monitoring of regional time-varying gravity field and ground stability based on CORS network [J]. *Science of Surveying and Mapping*, 2019, 44(6):29-36.
- [38] Zhao Jun, Gui Qingming. Global Robust Least Squares Estimation for Partial Variable Error Models [J]. *Acta Geodaetica et Cartographica Sinica*, 2016, 45(5):552-559.
- [39] Zhao, B., Bürgmann, R., Wang, D., Tan, K., Du, R., & Zhang, R. (2017). Dominant controls of downdip afterslip and viscous relaxation on the postseismic displacements following the Mw7.9 Gorkha, Nepal, earthquake, 122, 8376–8401. doi.org/10.1002/2017JB014366
- [40] Zhou Hang, Liu Lejun, Wang Dongliang, et al. The application of landslide monitoring system in Shanhou Village of the northern Changshan Island in landslide monitoring [J]. *Haiyang Xuebao*, 2016, 38(1): 124-132.